

Detecting Low Pass Graph Signals via Spectral Pattern: Sampling Complexity and Applications

Chenyue Zhang, Yiran He, Hoi-To Wai

Abstract—This paper proposes a blind detection problem for low pass graph signals. Without assuming knowledge of the exact graph topology, we aim to detect if a set of graph signal observations are generated from a low pass graph filter. Our problem is motivated by the widely adopted assumption of low pass (a.k.a. smooth) signals required by existing works in graph signal processing (GSP), as well as the longstanding problem of network dynamics identification. Focusing on detecting low pass graph signals on modular graphs whose cutoff frequency coincides with the number of clusters in the graph, we study and leverage the unique spectral pattern exhibited by such low pass graph signals to devise two detectors: one is based on Perron-Frobenius theorem, one is based on the K-means score. We analyze the sample complexity of these detectors considering the effects of graph filter’s properties, random delays, and other parameters. We show novel applications of the blind detector on robustifying graph learning, identifying antagonistic ties in opinion dynamics, and detecting anomalies in power systems. Numerical experiments validate our findings.

Index Terms—low pass graph filters, blind detection, sampling complexity, spectral pattern

I. INTRODUCTION

A growing trend in signal processing, machine learning, statistics is to develop tools for modeling and analyzing data defined on nodes of a graph, formally known as graph signals. Graphs encode the irregularly structured data and model the interactions between adjacent nodes. Such mathematical structure has found applications in social, financial, and biology networks [2]. An important problem is to understand the role of graph and its associated dynamics in data. While statistical methods such as graphical models [3] have been developed, recently popular GSP models have offered a promising approach that appeals to a wide range of data [4]–[6].

A fundamental building block of GSP is the linear graph filter which extends the classical linear time-invariant (LTI) filter from time domain to the node domain. It enables one to model graph signal as the output of a graph filter subject to excitation input. The graph filter acts as a black box that abstracts the complex network dynamics leading to the observations. Using this modeling philosophy, GSP algorithms have been developed for signal sampling, interpolation, graph topology learning, etc. [4]. They have been successfully applied to data from social networks, financial networks [7], brain activity dynamics [8], and physical networks [9].

A preliminary version of this work has been presented at ICASSP 2021 [1]. The authors are with the Department of SEEM, The Chinese University of Hong Kong, Shatin, Hong Kong SAR of China. E-mails: czhang@se.cuhk.edu.hk, yrhe@se.cuhk.edu.hk, htwai@se.cuhk.edu.hk. This work is supported in part by CUHK Direct Grant #4055135 and HKRGC Project #24203520.

Similar to LTI filters, linear graph filters may be classified as low pass, band pass, and high pass, in accord with its frequency response function [5]. In the GSP literature, low pass graph filters are usually assumed which lead to smooth graph signals that have similar signal values over adjacent nodes on the graph. Such *low pass or smooth* signal assumption has been a critical condition used for graph topology learning [10]–[13], blind community detection [14]–[17], centrality estimation [18]–[20], denoising [21], sampling [22], graph neural networks [23], [24]. On one hand, the low pass assumption can be justified using dynamics models from physics and social science [7]. On the other hand, without rigorous validation, the validity of the low pass assumption can be questionable. Example scenarios include when the system is under attack [25] or the observed data is corrupted [26].

To illustrate the risks in applying the above GSP works on non low pass data, e.g., corrupted data, we present a case study on graph topology learning from meteorology data using GL-SigRep [10]. The ‘clean’ dataset consists of the daily mean temperature in Netherlands from June 2020 to Feb 2023 on $N = 35$ stations and $M = 1000$ days of samples [available: <https://www.ecad.eu/>]. A corrupted dataset is formed by inserting noise into the clean dataset at random instances (see the caption of Fig. 1). The GL-SigRep algorithm [10] is applied to learn the weather station graph from the datasets. As the ground truth topology is unknown, we consider two evaluation metrics inspired by [10]. We first compare the similarity between the learnt graphs and a proximity graph constructed by assigning an edge between two stations if their distance is less than 125km. The area under ROC (AUROC) scores are 0.8258 (clean dataset), 0.4379 (corrupted dataset). The result for the clean dataset is consistent with the proximity graph, yet for the corrupted dataset, GL-SigRep may have learnt an erroneous graph. Next, we apply spectral clustering on the learnt graphs where the number of clusters K is determined by minimum descriptive length (MDL) [27]. As seen in Fig. 1, the clustering results from clean dataset are consistent with geography of the Netherlands which has low, flat lands in the west/north, and higher lands in the east/south; yet for corrupted dataset, the clustering result is inconclusive.

The above case study shows that applying GSP works on non low pass data without verifying the assumptions is risky as it may return inconclusive results that can harm downstream applications. As noted by [12], [13], a possible solution is to utilize alternative signal models. However this may incur other issues. For example, although the spectral template method [28] does not require smooth graph signals for topology

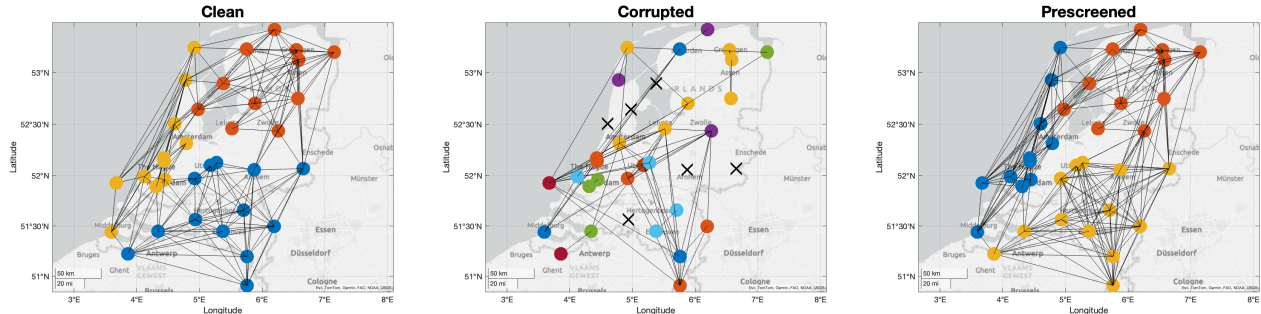


Fig. 1: **Graph topology learnt by GL-SigRep [10] and clustering results by spectral clustering** on the (Left) clean dataset, (Middle) corrupted dataset, (Right) pre-screened dataset. The corrupted observations are generated as 10 batches of ideal order-5 high pass signals, each with a duration $M_{ba} = 50$, and they are injected into the dataset at random positions; see (22). ‘X’ denotes the isolated nodes in the learnt graph. We set $m_{batch} = 50$ and $\delta = 0.65$ for the pre-screening procedure. The AUROCs compared to the proximity graph are 0.8258 (Clean) / 0.4379 (Corrupted) / 0.7597 (Pre-screened). With the MDL criterion, we found $K = 3$ clusters in the graphs learnt from clean and prescreened data.

learning, it has strict requirements on the excitation model and involves complex optimization criteria.

Instead of inventing new signal models, this work aims to *complement existing GSP works* by studying a blind detection problem which distinguishes if the given graph signals are low pass or not. Our work is motivated by two important aspects that have not been studied in the GSP community. (i) We devise a procedure to validate the low pass property in graph data required by GSP tools. (ii) We address a blind system identification problem by determining the type of graph filter followed by the graph data, and thus categorize the dynamics involved. As a preview application of our method, we apply the said procedure (see Sec. V) to prescreen the corrupted dataset in Fig. 1 and then run the GL-SigRep algorithm. The learnt graph achieves an AUROC score of 0.7597 compared to the proximity graph, and produces a clustering result that is consistent with the geography of the Netherlands.

Note that our blind detection problem is in general ill-posed due to the lack of exact graph topology knowledge. As a remedy, we concentrate on *modular* graphs consisting of a few densely connected components, i.e., a common case for social, biology, finance, physical networks [29]. Our idea lies in observing a unique *clustered spectral pattern* in the principal subspace spanned by low pass graph signals from modular graphs. Our contributions are:

- We develop blind detection methods for low pass graph signals through identifying the (dis)similarities between the low graph frequency subspace of the graph shift operators (GSO) and the principal subspace spanned by observed graph signals. We derive properties of the principal subspace spanned by low pass graph signals.
- We derive finite-sample performance bounds for the blind detectors when the graph (i) contains only one connected component with similar connection probability, (ii) is modular and contains K clusters following a stochastic block model (SBM) [30]. Our result shows that the detection performance improves with more nodes and/or the graph filters have sharper cutoffs. We also give insights for the detection performance applied to non-SBM graphs.
- We discuss applications utilizing the proposed detectors.

First, we design a prescreening scheme to robustify graph learning through removing non low pass graph signals from the dataset prior to applying graph learning. Second, we derive models for opinion dynamics with antagonistic relationships [31], [32] and power systems under data injection attack [33], [34]. Our detection method provides a data-driven evidence to discover such phenomena.

The proposed detection method takes its inspiration from recent works on blind graph feature learning. Examples are community detection [14]–[17], centrality estimation [18]–[20], equitable partitions [35], etc. These works derive knowledge from the principal signal subspace under the premise that the observations are low pass. In comparison, we take an *inverse problem* perspective by inquiring if a given set of graph signals are low pass. Notably, our development involves showing a *converse result* that the said spectral pattern cannot be found in non low pass signals.

Furthermore, this paper makes a first step towards *blind (topology-free) identification of unknown systems* [36] to *determine the type of dynamics* on a network. For example, the presence of antagonistic relationship in social networks result in an opinion formation process that can be described as non low pass graph filter; in power systems, data injection attacks result in graph signals of nodal voltages that are not low pass. In comparison, prior works on graph filter identification either utilize controlled perturbation experiments [37], [38], or require full knowledge of the graph topology [39], [40].

The rest of this paper is organized as follows. In Sec. II, we describe the observation model and the problem of detecting low pass graph filters. In Sec. III, we propose blind detection algorithm for the low pass graph signals. In Sec. IV, we analyze the sampling complexity of the proposed algorithms. Sec. V describes three new application examples for our algorithm. Sec. VI concludes the paper with numerical examples. Compared to the conference version [1], we consider low pass graph filters with high cutoff frequencies as well as providing a complete performance analysis. We also studied applications on detecting the network dynamics types.

II. PROBLEM STATEMENT

Consider an undirected, connected graph with N nodes given by $G = (V, E)$, where $V = [N] = \{1, \dots, N\}$ is the node set and $E \subseteq V \times V$ is the set of edges. The (weighted) adjacency matrix of G is a symmetric matrix defined by $\mathbf{A} = [A_{ij}]$ such that $A_{ij} > 0$ if $(i, j) \in E$, otherwise $A_{ij} = 0$. The normalized adjacency matrix is given by $\mathbf{A}_{\text{norm}} = \mathbf{D}^{-1/2} \mathbf{A} \mathbf{D}^{-1/2}$, where \mathbf{D} is the diagonal matrix with the i th diagonal element $d_i = \sum_{j=1}^N A_{ij}$, and the Laplacian matrix and normalized Laplacian matrix is defined by $\mathbf{L} = \mathbf{D} - \mathbf{A}$ and $\mathbf{L}_{\text{norm}} = \mathbf{I} - \mathbf{A}_{\text{norm}}$ respectively. A graph shift operator (GSO), denoted by \mathbb{S} , is a symmetric matrix such that $S_{ij} \neq 0$ only if $(i, j) \in E$ or $i = j$. For example, the (normalized) adjacency and Laplacian matrices are admissible GSOs. The GSO admits the eigenvalue decomposition $\mathbb{S} = \mathbf{V} \mathbf{\Lambda} \mathbf{V}^\top$, where the columns of $\mathbf{V} = (\mathbf{v}_1, \dots, \mathbf{v}_N)$ are the eigenvectors and $\mathbf{\Lambda} = \text{Diag}(\lambda_1, \dots, \lambda_N)$ is a diagonal matrix of the eigenvalues known as the *graph frequencies*. They are assumed to be distinct for simplicity, and are in ascending order as $\lambda_1 < \lambda_2 < \dots < \lambda_N$ for $\mathbb{S} \in \{\mathbf{L}, \mathbf{L}_{\text{norm}}\}$; or in descending order as $\lambda_1 > \lambda_2 > \dots > \lambda_N$ for $\mathbb{S} \in \{\mathbf{A}, \mathbf{A}_{\text{norm}}\}$.

We concentrate on the case where G is a *modular graph* [29], [41] with $K \ll N$ densely connected clusters¹. Mathematically, the modularity of G is characterized by the normalized cut: let $\mathcal{C}_1, \dots, \mathcal{C}_K$ be a partition of $[N]$,

$$\text{NCut}(\mathcal{C}_1, \dots, \mathcal{C}_K) = \sum_{k=1}^K \sum_{i \in \mathcal{C}_k} \sum_{j \notin \mathcal{C}_k} \frac{A_{ij}}{\sum_{\ell \in \mathcal{C}_k} \sum_{m \in [N]} A_{\ell m}}. \quad (1)$$

If $\text{NCut}_K^* := \min_{\mathcal{C}_1, \dots, \mathcal{C}_K} \text{NCut}(\mathcal{C}_1, \dots, \mathcal{C}_K) \approx 0$, we say that the graph is K -modular. Importantly, it is known that when $\mathbb{S} = \mathbf{L}_{\text{norm}}$, the condition $\text{NCut}_K^* \approx 0$ implies $\lambda_1, \dots, \lambda_K \approx 0$ [15], [42]. We notice that modular graphs are common in social, economics, biological networks [29]. On the other hand, the popular *SBM* is a generative random graph model that lead to modular graphs with high probability [43].

We consider linear graph filter as a continuous matrix function. Let $T_{\text{ord}} \in \mathbb{N} \cup \{\infty\}$ be the number of filter taps, a linear graph filter is described by [5]:

$$\mathcal{H}(\mathbb{S}) = \sum_{t=0}^{T_{\text{ord}}} h^{(t)} \mathbb{S}^t = \mathbf{V} h(\mathbf{\Lambda}) \mathbf{V}^\top = \mathbf{U} \mathbf{h} \mathbf{U}^\top, \quad (2)$$

where we have defined the frequency response function as $h(\lambda) = \sum_{t=0}^{T_{\text{ord}}} h^{(t)} \lambda^t$ and $h(\mathbf{\Lambda})$ is a diagonal matrix with the entries $\{h(\lambda_i)\}_{i=1}^N$. The diagonal matrix $\mathbf{h} := \text{Diag}(h_1, \dots, h_N)$ is composed of the eigenvalues for $\mathcal{H}(\mathbb{S})$ sorted as $|h_1| \geq |h_2| \geq \dots \geq |h_N|$, such that \mathbf{U} is the corresponding column re-ordered version of \mathbf{V} .

Note that $|h(\lambda)|$ measures amplification or attenuation of the energy of a graph signal at frequency λ . We observe the following definition for low pass graph filters [7]:

Definition 1. A graph filter $\mathcal{H}(\mathbb{S})$ is said to be K low pass if

$$\eta_K := \frac{\max_{i=K+1, \dots, N} |h(\lambda_i)|}{\min_{i=1, \dots, K} |h(\lambda_i)|} < 1. \quad (3)$$

¹The number of clusters depends on the nature of the network, e.g., for social networks with $N = 100$ to 1000 nodes, typically $K \leq 5$ [41], for biological networks with $N = 1000$ to 5000 nodes, typically $K \leq 50$.

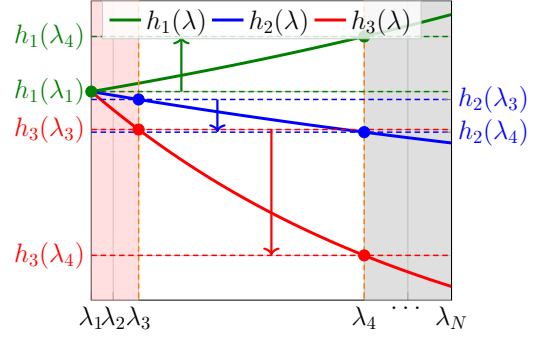


Fig. 2: Frequency responses $h(\lambda_i)$ against eigenvalue λ_i . (Green) $\mathcal{H}_1(\mathbf{L}) = (\mathbf{I} - 0.1\mathbf{L})^{-1}$, (Blue) $\mathcal{H}_2(\mathbf{L}) = (\mathbf{I} + 0.1\mathbf{L})^{-1}$ and (Red) $\mathcal{H}_3(\mathbf{L}) = \exp(-0.5\mathbf{L})$. The red shadow region indicates \mathbb{L}_{Low} region and the black shadow region indicates \mathbb{L}_{High} region. Note that $\mathcal{H}_2(\mathbf{L})$ and $\mathcal{H}_3(\mathbf{L})$ are $K = 3$ -low pass filters while $\mathcal{H}_1(\mathbf{L})$ is not [cf. Definition 1].

We refer our readers to the illustration in Fig. 2. The smaller η_K is, the ‘sharper’ the low pass filter is. The integer $K \in \{1, \dots, N-1\}$ represents the *cut off frequency*. Notice that the graph frequencies can be unevenly distributed. Take $\mathbb{S} = \mathbf{L}_{\text{norm}}$ as an example, a low pass frequency response function $h(\lambda)$ (e.g., a decreasing function in λ) is usually K -low pass if the underlying graph is *modular* with K densely connected components. Intuitively, this is because one has $\lambda_1, \dots, \lambda_K \approx 0$ in the ideal case while $\lambda_{K+1}, \dots, \lambda_N$ are bounded away from 0 [43] and $h(\lambda)$ is continuous in λ .

We consider the observation model where M filtered graph signals are obtained according to:

$$\mathbf{y}_m = \underbrace{\mathcal{H}(\mathbb{S}) \cdots \mathcal{H}(\mathbb{S})}_{J_m \text{ times}} \mathbf{x}_m + \mathbf{w}_m, \quad m = 1, \dots, M, \quad (4)$$

such that $\mathbf{x}_m \in \mathbb{R}^N$ is the excitation (a.k.a. input) signal and $\mathbf{w}_m \in \mathbb{R}^N$ is the observation or modeling noise. Moreover, the signal component of \mathbf{y}_m is the result of cascading J_m copies of $\mathcal{H}(\mathbb{S})$, which models the random delays in observations. This is motivated by the practical consideration where the delays may vary from sample to sample when acquiring the graph signals such as in rumor spreading; see [39, Sec. II-C]. Eq. (4) assumes a scenario that the observations/states on nodes following a dynamic process governed by the graph filter $\mathcal{H}(\mathbb{S})$. As a convention, we say that \mathbf{y}_m generated from (4) is a (K -)low pass graph signal with respect to (w.r.t.) \mathbb{S} when $\mathcal{H}(\mathbb{S})$ is (K -)low pass.

For simplified theoretical analysis, we assume that the observed signals are *stationary* [44], i.e., the excitation \mathbf{x}_m is zero-mean with covariance $\mathbf{C}_x = \mathbb{E}[\mathbf{x}_m \mathbf{x}_m^\top] = \mathbf{I}$. The observation noise is zero-mean with $\mathbb{E}[\mathbf{w}_m \mathbf{w}_m^\top] = \sigma^2 \mathbf{I}$. The delay J_m is uniformly distributed over $\{1, \dots, J\}$. Our detection methods can be readily applied even when $\mathbf{C}_x \neq \mathbf{I}$ and is possibly low rank; see the supplementary material.

A. Low Pass Graph Filter Detection Problem

Given a set of graph signals $\{\mathbf{y}_m\}_{m=1}^M$, we wish to determine if the signals are low pass or not w.r.t. \mathbb{S} . As mentioned, the problem can be easily solved if the GSO \mathbb{S} is known. For

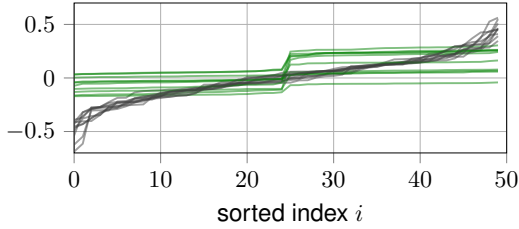


Fig. 3: Low pass (in green), non low pass (in black) graph signals generated from $\mathcal{H}(\mathbb{S})$ on an SBM graph with $K = 2$ clusters and $N = 50$ nodes. For each graph signal, we plot its elements sorted in ascending order. The *low pass signals* exhibit a *piecewise-constant* feature.

example, with noiseless observation, $J = 1$, we can estimate $|h(\lambda_i)|^2$ for each $i = 1, \dots, N$ through the periodogram $\mathbf{v}_i^\top \mathbb{E}[\mathbf{y}_m \mathbf{y}_m^\top] \mathbf{v}_i$ [45] and verifying Definition 1 directly.

Our aim is to tackle the detection problem in a *blind* setting where the GSO is unknown. This pertains to applications such as graph learning where the graph topology itself is the object to be estimated. However, the blind detection problem is *ill-posed* in general: a set of graph signals can be simultaneously *low pass* w.r.t. a graph while *not low pass* w.r.t. another graph.

Motivated by that many real networks graphs tend to be *modular* [29] [cf. (1)], we inquire if such graphs can lead to any discernible pattern in the low pass and non low pass graph signals generated. Fig. 3 shows the ensemble of low pass, non low pass signals generated on a modular (SBM) graph with $N = 50$ nodes. Here, the low pass graph signals generated show a unique pattern *not found* in the non low pass signals: upon a simple sorting, the graph signal is almost *piecewise constant*. The demonstrated pattern suggests that *under the premises of modular graph with $K \geq 1$ clusters, where K is known, the blind detection problem for K low pass graph signals can be solvable*. Formally, our main problem is:

Problem 1. *Given the number of clusters K , and a set of graph signals $\{\mathbf{y}_m\}_{m=1}^M$ generated from (4), we determine if the underlying graph filter $\mathcal{H}(\mathbb{S})$ is K -low pass.*

Denote $\mathcal{T}_{\text{gnd}} \in \{\mathcal{T}_0, \mathcal{T}_1\}$ as the ground truth hypothesis, where

- \mathcal{T}_0 : the null hypothesis refers to when $\mathcal{H}(\mathbb{S})$ is K low pass;
- \mathcal{T}_1 : the alternate hypothesis refers to when $\mathcal{H}(\mathbb{S})$ is *not* K low pass (may be bandpass, high pass, etc.).

As an extension, one may wish to consider the alternate hypothesis \mathcal{T}_1 which includes *any graph signals that are not generated by (4) with K -low pass filter* and null hypothesis \mathcal{T}_0 with K -low pass signals on non-modular graphs. Nevertheless, we found empirically that our detector(s) is effective in detecting signals that are not generated by (4).

III. DETECTING LOW PASS GRAPH SIGNALS

We begin our endeavor by analyzing the covariance matrix of (4). Observe that

$$\mathbf{C}_y = \mathbb{E}[\mathbf{y}_m \mathbf{y}_m^\top] = \frac{1}{J} \sum_{\tau=1}^J [\mathcal{H}(\mathbb{S})]^{2\tau} + \sigma^2 \mathbf{I}, \quad (5)$$

where the noiseless covariance is

$$\bar{\mathbf{C}}_y = \frac{1}{J} \sum_{\tau=1}^J [\mathcal{H}(\mathbb{S})]^{2\tau} = \mathbf{V} \left(\frac{1}{J} \sum_{\tau=1}^J h(\Lambda)^{2\tau} \right) \mathbf{V}^\top. \quad (6)$$

Denote the *top- K eigenvectors* of $\bar{\mathbf{C}}_y$ as \mathbf{U}_K . If $\mathcal{H}(\mathbb{S})$ is K low pass, it is clear that \mathbf{U}_K spans the same subspace as $\text{span}\{\mathbf{v}_1, \dots, \mathbf{v}_K\}$, i.e., the eigenvectors of \mathbb{S} corresponding to the K lowest graph frequencies; otherwise if $\mathcal{H}(\mathbb{S})$ is *not* K -low pass, the subspace spanned by \mathbf{U}_K contains one or more eigenvectors from $\{\mathbf{v}_{K+1}, \dots, \mathbf{v}_N\}$ of \mathbb{S} .

Our idea to handle Problem 1 is to verify *whether the K -dimensional principal subspace of \mathbf{C}_y coincides with a particular structure in $\text{span}\{\mathbf{v}_1, \dots, \mathbf{v}_K\}$* which we refer to as the *spectral pattern* of low pass signals. In the sequel, we show that these structures can be exposed upon careful observations. The study is divided into two cases depending on the number of clusters in the graph.

Case of $K = 1$: We first focus on the case when it is known that the graph G is *non-modular* (with $K = 1$). Problem 1 in this case aims at detecting graph signals that are 1-low pass. The development hinges on a well-known property for \mathbf{v}_1 :

Proposition 1. *Let G be connected. The eigenvector corresponding to the lowest graph frequency, \mathbf{v}_1 , is the only positive eigenvector² of \mathbf{L}_{norm} , \mathbf{L} , \mathbf{A}_{norm} , \mathbf{A} . For $i \geq 2$, the eigenvector \mathbf{v}_i must have at least one positive and negative element.*

This proposition is a direct consequence of the Perron-Frobenius theorem; see Appendix B.

Despite its simplicity, Proposition 1 illustrates a *sufficient and necessary* condition for detecting 1-low pass signals. When $\mathcal{H}(\mathbb{S})$ is 1 low pass, the top eigenvector \mathbf{u}_1 of the noiseless covariance $\bar{\mathbf{C}}_y$ is the *only* positive eigenvector; yet when $\mathcal{H}(\mathbb{S})$ is *not* 1 low pass, \mathbf{u}_1 has at least one positive and negative element. Consider the function:

$$\text{Pos}(\mathbf{u}) := \min\{\|(\mathbf{u})_+ - \mathbf{u}\|_1, \|(-\mathbf{u})_+ + \mathbf{u}\|_1\}, \quad (7)$$

where $(\mathbf{u})_+ := \max\{\mathbf{0}, \mathbf{u}\}$, and the function outputs zero if and only if \mathbf{u} is a positive (or negative) vector. Subsequently, the proposed detector in Algorithm 1 is a direct application of the above principle which checks if $\hat{\mathbf{u}}_1$ from the sampled covariance $\hat{\mathbf{C}}_y^M$ is the most positive eigenvector.

Case of $K \geq 2$: We consider the case when the graph is modular with K densely connected clusters. Problem 1 in this case refers to detecting K -low pass graph signals. For simplicity, we fix $\mathbb{S} = \mathbf{L}_{\text{norm}}$ as the GSO in the following discussions. Notice that both our detection method and analysis can be applied to other choice of GSOs.

We study $\{\mathbf{v}_1, \dots, \mathbf{v}_K\}$ *as well as* the bulk eigenvectors $\{\mathbf{v}_{K+1}, \dots, \mathbf{v}_N\}$. Unlike the previous case, the spectral pattern of $\{\mathbf{v}_2, \dots, \mathbf{v}_K\}$ may not be obvious at the first glance, where the eigenvectors' elements fluctuate between positive and negative values. Fig. 4 (left) shows the *sorted* and *unsorted* eigenvectors of $\mathbb{S} = \mathbf{L}_{\text{norm}}$ for a modular (SBM) graph with $K = 3$ clusters. *Upon sorting*, the principal eigenvectors $\mathbf{v}_1, \mathbf{v}_2, \mathbf{v}_3$ exhibit a piece-wise constant behavior; while it is not the case for bulk eigenvectors $\mathbf{v}_4, \mathbf{v}_5, \dots$. We should mention that the above phenomena has been observed [42] for modular graphs where for $\ell = 1, \dots, K$, the elements of

²Note that both $\mathbf{v}_1, -\mathbf{v}_1$ are eigenvectors with the eigenvalue λ_1 . We assume $\mathbf{v}_1 > \mathbf{0}$ to avoid such ambiguity.

Algorithm 1 Tackling Problem 1

- 1: **INPUT:** Observed graph signals $\{\mathbf{y}_m\}_{m=1}^M$, no. of clusters in the graph K , threshold parameter δ .
- 2: Evaluate $\widehat{\mathbf{C}}_y^M = (1/M) \sum_{m=1}^M \mathbf{y}_m \mathbf{y}_m^\top$.
- 3: Compute the eigenvalue decomposition (EVD) of $\widehat{\mathbf{C}}_y^M$ as $\widehat{\mathbf{U}} \widehat{\Lambda} \widehat{\mathbf{U}}^\top$, where the eigenvectors $\widehat{\mathbf{u}}_1, \dots, \widehat{\mathbf{u}}_N$ are sorted in descending order with the eigenvalues.
- 4: **If** $K = 1$, perform the detection as

$$\widehat{\mathcal{T}} = \begin{cases} \mathcal{T}_0, & \text{if } \text{Pos}(\widehat{\mathbf{u}}_1) < \min_{j=2, \dots, N} \text{Pos}(\widehat{\mathbf{u}}_j), \\ \mathcal{T}_1, & \text{otherwise.} \end{cases} \quad (8)$$

- 5: **If** $K \geq 2$, perform the detection as

$$\widehat{\mathcal{T}} = \begin{cases} \mathcal{T}_0, & \text{if } \mathbb{K}([\widehat{\mathbf{u}}_1, \dots, \widehat{\mathbf{u}}_K]) < \delta, \\ \mathcal{T}_1, & \text{otherwise,} \end{cases} \quad (9)$$

where $\mathbb{K}(\cdot)$ is defined in (10).

- 6: **OUTPUT:** the estimated hypothesis $\widehat{\mathcal{T}}$.
-

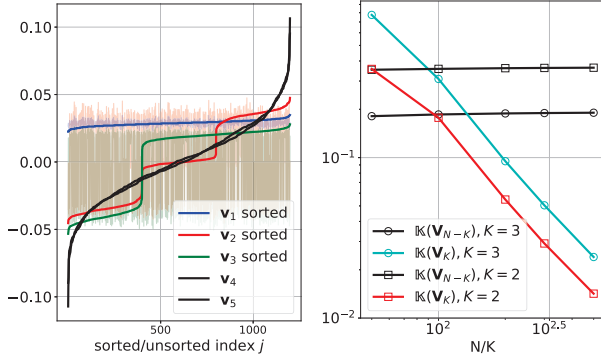


Fig. 4: (Left) Eigenvectors of \mathbf{L}_{norm} where the underlying graph contains $K = 3$ clusters. Paled colors denote unsorted eigenvectors. (Right) K -means score $\mathbb{K}(\mathbf{V}_K)$ and that of last $N - K$ eigenvectors $(N - K)^{-1} \sum_{i=K+1}^N \mathbb{K}(\mathbf{v}_i)$ against N/K .

\mathbf{v}_ℓ will be ‘flat’ over the cluster, i.e., $[\mathbf{v}_\ell]_{i,:} \approx [\mathbf{v}_\ell]_{j,:}$ for all nodes i, j belonging to the same cluster; and it has been shown analytically for stochastic block models [30], [43], [46], [47].

Together with (6), our observations suggest that low pass signals lead to covariance matrix with *clusterable principal eigenvectors*. To detect such pattern, a natural choice is to apply the K -means score to measure the degree of (non) low pass-ness. For any matrix $\mathbf{N} \in \mathbb{R}^{N \times K}$, define the score:

$$\mathbb{K}(\mathbf{N}) := \min_{\substack{S_i \cap S_j = \emptyset, i \neq j \\ S_1 \cup \dots \cup S_K = V}} \sum_{i=1}^K \sum_{\ell \in S_i} \left\| \mathbf{n}_\ell - \frac{1}{|S_i|} \sum_{j \in S_i} \mathbf{n}_j \right\|^2, \quad (10)$$

where $\mathbf{n}_\ell \in \mathbb{R}^K$ is the ℓ th row of \mathbf{N} . The minimization can be effectively handled by the standard K -means procedure [48].

We observe that when $\mathcal{H}(\mathbb{S})$ is K -low pass, one has $\text{span}\{\widehat{\mathbf{U}}_K\} \approx \text{span}\{\mathbf{v}_1, \dots, \mathbf{v}_K\}$ and thus $\mathbb{K}(\widehat{\mathbf{U}}_K)$ is small; vice versa, when $\mathcal{H}(\mathbb{S})$ is not K -low pass, $\widehat{\mathbf{U}}_K$ contains at least one eigenvector from the bulk $\{\mathbf{v}_{K+1}, \dots, \mathbf{v}_N\}$ and the score $\mathbb{K}(\widehat{\mathbf{U}}_K)$ is large as at least one of the eigenvectors is not clusterable. Finally, this suggests a threshold detector

on $\mathbb{K}(\widehat{\mathbf{U}}_K)$ in Algorithm 1. Although the detector shares the same ingredient with clustering algorithms such as spectral clustering [42] in applying the K -means score metric (10), our goals are different. We aim to measure how the principal eigenvectors of $\widehat{\mathbf{C}}_y^M$ are aligned with $\text{span}\{\mathbf{v}_1, \dots, \mathbf{v}_K\}$, via (10) which is akin to performing a clusterability analysis [49].

Thus far, we have only presented empirical insights to derive the blind detector. To justify the correctness of Algorithm 1, it is necessary to impose further structure on the detection problem. Below, we analyze an *idealized* modular graph model of G yielded by the planted partition SBM.

Definition 2. [30] Let $p, r > 0$, $p + r \leq 1$. We denote $G \sim \text{SBM}(K, N, r, p)$ as the random graph with N nodes that are partitioned into K equal sized blocks $\mathcal{C}_1, \dots, \mathcal{C}_K$ ³. The edges are generated independently and randomly according to:

$$\Pr[(i, j) \in E] = \begin{cases} p + r & , \text{if } i \in \mathcal{C}_k, j \in \mathcal{C}_k, \\ r & , \text{if } i \in \mathcal{C}_k, j \in \mathcal{C}_\ell, k \neq \ell. \end{cases} \quad (11)$$

Take $\mathbb{S} = \mathbf{L}_{\text{norm}}$. We shall verify two properties: (i) $\mathbb{K}(\mathbf{N}) \approx 0$ when \mathbf{N} is a column permuted version of \mathbf{V}_K , (ii) $\mathbb{K}(\mathbf{N})$ is bounded away from zero when \mathbf{N} contains at least one eigenvector from $\{\mathbf{v}_{K+1}, \dots, \mathbf{v}_N\}$.

The first property is confirmed by the proposition:

Proposition 2. Let $G \sim \text{SBM}(K, N, r, p)$ with $p \geq r > 0$, $\frac{p}{K} + r \geq \frac{32 \log N + 1}{N}$, and take $\mathbb{S} = \mathbf{L}_{\text{norm}}$ with unweighted adjacency matrix. Then, with probability at least $1 - 2/N$,

$$\mathbb{K}(\mathbf{N}) \leq \frac{35^2 K^3 \log N}{p(N - K)} \quad (12)$$

for any \mathbf{N} given by permuting the columns of \mathbf{V}_K .

The proof, which is due to [50], can be found in Appendix F.

For the second property where the columns of \mathbf{N} contain at least one eigenvector from $\{\mathbf{v}_{K+1}, \dots, \mathbf{v}_N\}$, we provide a partial answer motivated by empirical studies. To this end, in Fig. 4 (right) we simulate the K -means scores on the eigenvectors $\mathbb{K}(\mathbf{v}_\ell)$, $\ell = 1, \dots, N$, of \mathbf{L}_{norm} averaged from $M = 500$ realizations of $G \sim \text{SBM}(K, N, \log(N)/N, 0.1)$. Observe that $\mathbb{K}(\mathbf{V}_K)$ decreases as $\mathcal{O}(1/N)$, while for $\ell = K + 1, \dots, N$, $\mathbb{K}(\mathbf{v}_\ell)$ remains bounded from below by a constant. This leads to the following assumption:

H1. For $N \gg K$. Let $G \sim \text{SBM}(K, N, r, p)$ and denote \mathbf{v}_ℓ as the ℓ th largest eigenvector of the corresponding \mathbf{L}_{norm} . There exists a constant c_{SBM} independent of N, p, r such that $\mathbb{K}(\mathbf{v}_\ell) \geq c_{\text{SBM}} > 0$, $\ell = K + 1, \dots, N$.

To our best knowledge, proving the above assumption is an open research problem. We refer the readers to works on bulk eigenvectors in SBMs for partial results that affirm the conjecture: [51], [52] applied random matrix theory to show that the elements of the bulk eigenvectors \mathbf{v}_ℓ , $\ell = K + 1, \dots, N$ follow a near-Gaussian distribution that would lead to H1.

³For simplicity, assume that N is divisible by K .

Now, suppose that at least one of the column vectors in \mathbf{N} is a bulk eigenvector, \mathbf{v}_ℓ , $\ell \in \{K+1, \dots, N\}$, of \mathbf{L}_{norm} . Under H1, we have

$$\begin{aligned} \mathbb{K}(\mathbf{N}) &\geq \mathbb{K}(\mathbf{n}_1^{\text{col}}) + \dots + \mathbb{K}(\mathbf{n}_K^{\text{col}}) \\ &\geq \mathbb{K}(\mathbf{n}_i^{\text{col}}) = \mathbb{K}(\mathbf{v}_\ell) \geq c_{\text{SBM}} > 0, \end{aligned} \quad (13)$$

where $\mathbf{n}_i^{\text{col}}$ denotes the i th column of \mathbf{N} . Combining with properties (i) and (ii), we conclude that as $\widehat{\mathbf{U}}_K$ can be modeled with the above cases for \mathbf{N} when $M \rightarrow \infty$ and $\sigma \rightarrow 0$, thresholding on $\mathbb{K}(\widehat{\mathbf{U}}_K)$ detects if $\mathcal{H}(\mathbb{S})$ is low pass or not.

Remark 1. Solving Problem 1 requires knowledge on the number of clusters K . For a number of applications, the latter is known a-priori, e.g., the graph of US Senate is believed to have $K = 2$ due to the bipartisan nature. Otherwise, we apply a heuristic procedure extended from Algorithm 1: set $\hat{K} = 1$,

- 1) If $\hat{K}^{-1} \mathbb{K}(\widehat{\mathbf{U}}_{\hat{K}}) < \delta_{\text{Est}}$, then declare that the graph filter is \hat{K} low pass; otherwise, go to step 2.
- 2) If $\hat{K} > K_0$, declare that the graph filter is not low pass; otherwise, set $\hat{K} = \hat{K} + 1$.

In the above, δ_{Est} , K_0 respectively denote the threshold parameter and estimate on the maximum number of clusters.

IV. FINITE-SAMPLE PERFORMANCE ANALYSIS

This section analyzes the performance of proposed algorithm when the number of samples M is finite. In a nutshell, our analysis relies on the fact that the eigenvectors of \mathbf{C}_y are re-ordered version of the GSO's eigenvectors [cf. (6)]. It suffices to estimate the number of samples required for the spectral pattern to emerge via the Davis-Kahan theorem.

To facilitate our analysis, let us consider the assumption:

H2. The magnitudes of frequency response are distinct at all graph frequencies, i.e., $|h(\lambda_i)| \neq |h(\lambda_j)|$ for all $i \neq j$.

This assumption is easy to satisfy, e.g., it holds when $\lambda_i \neq \lambda_j$ and $h(\cdot)$ is a strict monotonic function. Under \mathcal{T}_0 , the matrix \mathbf{U}_K is a column-permuted version of $\mathbf{V}_K = (\mathbf{v}_1 \cdots \mathbf{v}_K)$. Let us also define a few quantities on the eigenvalues of $\overline{\mathbf{C}}_y$. Set as the j th eigengap for $\overline{\mathbf{C}}_y$

$$\Delta\beta_j := \beta_j(\overline{\mathbf{C}}_y) - \beta_{j+1}(\overline{\mathbf{C}}_y), \quad j = 1, \dots, N-1, \quad (14)$$

and $\Delta\beta_0 = \infty$, where $\beta_j(\overline{\mathbf{C}}_y)$ denotes the j -th largest eigenvalue of $\overline{\mathbf{C}}_y$. To get insights, we recall that h_j is the j th largest entry in the set of filter frequency responses $\{|h(\lambda_1)|, \dots, |h(\lambda_N)|\}$. Observe that

$$\Delta\beta_j = \frac{1}{j} \sum_{\tau=1}^j (h_j^{2\tau} - h_{j+1}^{2\tau}), \quad (15)$$

where the j th eigengap depend on the frequency response of the graph filter. For example with K low pass filter defined on K clusters graphs, as the frequency response maybe flat before the cutoff frequency at λ_K , we expect $\Delta\beta_K$ to be large, and is in fact, proportional to the reciprocal of low pass ratio $1/\eta_K$, while $\{\Delta\beta_j\}_{j=1}^{K-1}$ is small. In other words, these constants directly measure the ‘sharpness’ of the graph filter across different graph frequencies.

Case of $K = 1$. In this case, Algorithm 1 relies on the positivity function (7) applied to the top eigenvector of \mathbf{C}_y . We observe the sampling complexity bound:

Theorem 1. Assume that there exists constants $c_0, \overline{\Delta}$ such that the graph filters of interest (under \mathcal{T}_0 or \mathcal{T}_1) satisfy

$$0 < c_0 \leq \min_{j=2, \dots, N} \text{Pos}(\mathbf{v}_j), \quad 0 < \overline{\Delta} \leq \min_{j=1, \dots, N-1} \Delta\beta_j \quad (16)$$

and the noise variance satisfies $\sigma^2 \sqrt{N} < 2^{-2.5} c_0 \overline{\Delta}$. If the number of samples M satisfies

$$\sqrt{\frac{M}{\log M}} \geq \frac{2c_1 \text{tr}(\mathbf{C}_y)}{2^{-2.5} c_0 \overline{\Delta} / \sqrt{N} - \sigma^2}, \quad (17)$$

where c_1 is a constant independent of N, M , then it holds $\Pr(\widehat{\mathcal{T}} = \mathcal{T}_{\text{gnd}}) \geq 1 - 10/M$, where the randomness is due to sampling from (4).

The proof is relegated to Appendix D.

The constants c_0, Δ_{min} inform the class of admissible (low pass or non-low pass) graph filters and its underlying GSO that are detectable by Algorithm 1 with enough samples. In particular, the constant c_0 denotes the spread of the values in non-principal eigenvector \mathbf{v}_j of admissible GSOs. There are normally $\Theta(N)$ negative elements in \mathbf{v}_j as deduced in [53], implying $c_0 = \Theta(\sqrt{N})$. Thus, the denominator is positive with $\sigma^2 = \mathcal{O}(\overline{\Delta})$. On the other hand, the constant $\overline{\Delta}$ depends on the class of admissible graphs and the ‘sharpness’ of the graph filters defined on them as discussed in (15). It is bounded away from zero since the graph only has $K = 1$ cluster. We deduce that the number of samples M required for correct detection decreases with small σ , $\text{tr}(\mathbf{C}_y)$.

Case of $K \geq 2$. The analysis for detecting low pass graph filters with high cutoff frequency ($K \geq 2$) is more involved since the graph filters may have frequency response that are non-monotone in λ .

We obtain the sampling complexity bound for Algorithm 1:

Theorem 2. Let $G \sim \text{SBM}(K, N, r, p)$ with $p \geq r > 0$, $\frac{p}{K} + r \geq \frac{32 \log N + 1}{N}$ and take $\mathbb{S} = \mathbf{L}_{\text{norm}}$ with unweighted adjacency matrix. Accordingly, we denote the classes of K -low pass and non K -low pass graph filters as $\mathcal{H}_{\mathbb{S}}^{\text{low}}, \mathcal{H}_{\mathbb{S}}^{\text{hi}}$, respectively. Assume that

$$\overline{\Delta} := \inf_{\Delta\beta_K \cdot \mathcal{H}(\mathbb{S}) \in \mathcal{H}_{\mathbb{S}}^{\text{low}} \cup \mathcal{H}_{\mathbb{S}}^{\text{hi}}} \Delta\beta_K > 0, \quad (18)$$

the following threshold-dependent constant:

$$\tilde{\delta}_{\text{min}} := \min \left\{ \sqrt{\frac{\delta}{2} - \frac{1225K^3 \log N}{p(N-K)}}, \sqrt{c_{\text{sbm}}} - \sqrt{\delta} \right\} > 0, \quad (19)$$

and the noise variance satisfies $\sigma^2 \leq \tilde{\delta}_{\text{min}} \overline{\Delta} / \sqrt{8K}$. If the number of samples M satisfies

$$\sqrt{\frac{M}{\log M}} \geq \frac{2c_1 \text{tr}(\mathbf{C}_y)}{\tilde{\delta}_{\text{min}} \overline{\Delta} / \sqrt{8K} - \sigma^2}, \quad (20)$$

where c_1 is a constant independent of N, M to be defined later in Lemma 3, then it holds $\Pr(\widehat{\mathcal{T}} = \mathcal{T}_{\text{gnd}}) \geq 1 - 10/M - 2/N$,

where the randomness is due to sampling from (4) and $G \sim \text{SBM}(K, N, r, p)$.

The proof is relegated to Appendix E. Note that when $K = 1$, $\bar{\Delta}$ defined in (18) also satisfies the second inequality in (16).

The constants $\bar{\Delta}, \tilde{\delta}_{\min}$ characterize the class of K low pass or non K low pass graph filters detectable by Algorithm 1 upon accruing a sufficient number of samples. In specific, $\tilde{\delta}_{\min}$ depends on the user defined threshold value δ in Algorithm 1. If N is large, and the clusters are dense (due to p) with sparse inter-cluster connections (due to $r + p \leq 1$), we can set $\delta = \Theta(1)$ which leads to $\tilde{\delta}_{\min} = \Theta(1)$. On the other hand, $\bar{\Delta}$ in (18) depends on the ‘sharpness’ of the admissible graph filters. As the sample complexity (20) is inversely proportional to $\bar{\Delta}$, less samples will be required to correctly detect the graph filter if the admissible graph filters are ‘sharper’ at the cutoff frequencies. With a sufficiently small noise variance and large N, M , Algorithm 1 is guaranteed to solve Problem 1.

Finally, we estimate the sampling complexity of Algorithm 1 from (17), (20). Particularly, with sufficiently small noise σ^2 and large N , our theorems show that the *minimum number of samples required for correct detection with high probability* satisfies:

$$\sqrt{M/\log M} = \Omega(\bar{\Delta}^{-1}\sqrt{K}). \quad (21)$$

As $\bar{\Delta}$ is large for ‘sharp’ graph filters, i.e., it is proportional to $1/\eta_K$ for small η_K with low pass graph filters, we anticipate that the detection performance improves for (i) graphs with few number of clusters and (ii) the graph filters to be detected have sharp cutoffs.

Remark 2. *The above result has concentrated on $G \sim \text{SBM}(K, N, r, p)$ and $\mathbb{S} = \mathbf{L}_{\text{norm}}$. As mentioned, the choice of SBM model illustrates the performance of Algorithm 1 in an ideal model. In practice, it gives insights that the detection performance improves when the underlying graph has dense clusters and sparse inter-cluster connections.*

V. APPLICATION EXAMPLES

Tackling Problem 1 is a critical step for downstream GSP applications pertaining to graph data. This section describes examples to illustrate the applications of proposed algorithms in (i) robustifying graph learning, (ii) detecting the sign-ness of opinion dynamics in social networks, and (iii) detecting anomalies for power networks.

A. Robustifying Graph Learning

Graph learning is a longstanding problem in GSP, whose aim is to infer the graph topology from graph signal observations [12], [13]. Among others, a popular setup is to model observations as *smooth graph signals*, i.e., low pass graph signals [11], [54]. In reality, the observations can occasionally be corrupted by *outliers*. In light of this, robust graph learning algorithms have been recently proposed, e.g., [55] for an inpainting approach, [56] applied distributional robust optimization, and [57] for an outlier-resilient algorithm.

Our idea is to model the graph signals as being occasionally corrupted with a non low pass signal \mathbf{p}_m . Let $\mathcal{H}(\mathbb{S})$ be a low pass graph filter, for $m = 1, \dots, M$,

$$\mathbf{y}_m = \begin{cases} \mathcal{H}(\mathbb{S})\mathbf{x}_m + \mathbf{w}_m & , m \in \mathcal{M}_{\text{clean}}, \\ \mathbf{p}_m + \mathbf{w}_m & , m \in \mathcal{M}_{\text{pollut}}, \end{cases} \quad (22)$$

where $\mathcal{M}_{\text{clean}}, \mathcal{M}_{\text{pollut}}$ partitions the set $[M] = \{1, \dots, M\}$, and \mathbf{w}_m is the modeling/observation noise. Notice that (22) is inspired by [55] when the sampling set is small and selected randomly. Since the outlier signals can be due to anomalous sensor measurements or missing data [26], (22) models the practical scenario when these events persist for a short period of time and recover afterwards. It is suggested to model the outlier signals as non low pass (i.e., high pass) signals on graph filters w.r.t. possibly time varying GSO [7]. For example, the latter can be modeled as $\mathbf{p}_m = \mathcal{H}_{\text{HP}}(\mathbb{S})\mathbf{x}_m$, where $\mathcal{H}_{\text{HP}}(\cdot)$ corresponds to a non low pass filter violating Definition 1; or it can be modeled as a contaminated signal $\mathbf{p}_m = \mathcal{H}(\mathbb{S})\mathbf{x}_m + \Delta\mathbf{p}_m$ with $\Delta\mathbf{p}_m$ being a sparse vector.

From Fig. 1 (middle), we recall that learning the graph topology directly from (22) via methods like GL-SigRep [54] can produce inconclusive result. To this end, we propose a simple solution that pre-screens the dataset by removing corrupted signals using Algorithm 1. Let m_{batch} be the batch size such that there are $M_{\text{batch}} = M/m_{\text{batch}}$ batches. Assuming that K is known, we apply

- 1) For $b = 1, \dots, M_{\text{batch}}$, apply Algorithm 1 on \mathbf{y}_m , $m = (b-1)m_{\text{batch}} + 1, \dots, bm_{\text{batch}}$. Remove the batch if the involved signals are not K low pass.
- 2) Apply graph learning method such as GL-SigRep [54] or SpecTemp [28] on the remaining graph signals.

Fig. 1 (right) demonstrated the efficacy of the pre-screened graph learning procedure (via GL-SigRep) above. We remark that the parameter m_{batch} trades off between the accuracy of pre-screening and performance of graph learning. The success of the procedure hinges on whether $\mathcal{M}_{\text{pollut}}$ is a rare event or not; see Sec. VI for a detailed study.

B. Detecting Signed Opinion Dynamics

Signed graph is a common model for social networks with cooperative (trust/friendly) and antagonistic (distrust/hostile) relationships [31]. We set $G_s = (V, E^+, E^-)$, where $V = \{1, \dots, N\}$ denotes the set of agents, $E^+, E^- \subseteq V \times V$ denote the positive, negative edge sets such that $E^+ \cap E^- = \emptyset$. Accordingly, the graph is endowed with two adjacency matrices \mathbf{A}_{E^+} and \mathbf{A}_{E^-} , such that $[\mathbf{A}_{E^+}]_{i,j} > 0$ iff $(i, j) \in E^+$ and $[\mathbf{A}_{E^-}]_{i,j} < 0$ iff $(i, j) \in E^-$, otherwise $[\mathbf{A}_{E^+}]_{i,j} = [\mathbf{A}_{E^-}]_{i,j} = 0$. We notice that signed graph learning can be achieved using classical algorithms such as [58] through accounting anti-correlations in data, and recent papers have proposed improved algorithms on the topic [59]–[61].

From a system identification point of view, a relevant problem is to inquire *if a social network is dominated with antagonistic relationships through observing opinion data*. We demonstrate that this problem can be approximated as a special case of Problem 1, and therefore Algorithm 1 can be applied.

Our model is based on that of Altafini [32] for the opinion formation process (see [62] for a survey involving signed graphs) together with R stubborn agents whose opinions are unaffected by others [63], [64]. The latter represent entities who inject opinions into the social network. Let $\mathbf{y}_m(\tau)$, $\mathbf{z}_m(\tau)$ be opinions of regular, stubborn agents at time τ , we have:

$$\mathbf{y}_m(\tau + 1) = \alpha(\mathbf{A}_{E^+} + \mathbf{A}_{E^-})\mathbf{y}_m(\tau) + (1 - \alpha)\mathbf{B}\mathbf{z}_m, \quad (23)$$

where $\alpha \in (0, 1)$ and $\mathbf{B} \in \mathbb{R}^{N \times R}$ represents the mutual trust/distrust between stubborn and regular agents. Assume normalized weighted adjacency matrices such that $|\mathbf{A}_{E^+} + \mathbf{A}_{E^-}|\mathbf{1} = \mathbf{1}$ and $[\alpha(\mathbf{A}_{E^+} + \mathbf{A}_{E^-}), (1 - \alpha)\mathbf{B}]\mathbf{1} = \mathbf{1}$. The recursion (23) is stable and admits an equilibrium state:

$$\mathbf{y} = (1 - \alpha)(\mathbf{I} - \alpha(\mathbf{A}_{E^+} + \mathbf{A}_{E^-}))^{-1}\mathbf{B}\mathbf{z}. \quad (24)$$

Notice that our signal model in Sec. II was defined only for *unsigned graphs*. To analyze (24), we utilize an *unsigned surrogate adjacency matrix* for G_s as the GSO matrix $\mathbb{S} = \bar{\mathbf{A}} = \mathbf{A}_{E^+} - \mathbf{A}_{E^-}$, representing an unsigned surrogate graph $G = (V, E^+ \cup E^-)$. We observe three cases:

- 1) When all edges are positive, (24) is the output of graph filter $\mathcal{H}(\mathbb{S}) = (\mathbf{I} - \alpha\mathbb{S})^{-1}$ with the excitation $(1 - \alpha)\mathbf{B}\mathbf{z}$. These are K -low pass graph signals [7].
- 2) When all edges are negative, (24) is the output of graph filter $\mathcal{H}(\mathbb{S}) = (\mathbf{I} + \alpha\mathbb{S})^{-1}$. In this case, the graph signals are *not* K -low pass.
- 3) When there are both positive and negative edges, it can be shown using a simple Taylor approximation that

$$\begin{aligned} \mathcal{H}(\mathbb{S}) &= (\mathbf{I} - \alpha(\mathbb{S} + 2|\mathbf{A}_{E^-}|))^{-1} \\ &\approx (\mathbf{I} - \alpha\mathbb{S})^{-1} + \mathcal{O}(\alpha\|\mathbf{A}_{E^-}\|). \end{aligned} \quad (25)$$

The number/strength of negative edges influence the low pass property of $\mathcal{H}(\mathbb{S})$.

Recall that the metrics $\text{Pos}(\hat{\mathbf{u}}_1)$ or $\mathbb{K}(\hat{\mathbf{U}}_K)$ in Algorithm 1 estimates the level of *low-pass-ness* for a set of graph signals. Combined with the observations above, they measure the strength of *antagonistic relationships* in a social network.

We remark that our approach differs from recent studies on signed GSP, e.g., [59]. For given graph signals, our aim is to detect if the graph is *signed or not* without knowing the graph topology, while signed GSP considers the frequency analysis of the signals defined on the signed graph, where the latter topology and the signs of edges are known a-priori.

C. Detecting Anomalies in Power Networks

An important task in power system is to protect the latter against *false data injection attack* (FDIA) which may obfuscate power system state estimator and lead to unstable behavior. As the power system operations are dependent on the grid of transmission lines and buses, GSP-derived anomaly detectors have been studied in a number of prior works [33], [34]. Most of these detectors require knowledge of the grid's topology. While the latter's knowledge is usually available since the power system is man-made, in some scenarios, its topology may not be precisely estimated when the grid is energized [65], e.g., some power lines may not be operational.

Similar to the previous application example, our aim is to showcase that FDIA detection can be cast as a special case of Problem 1, where we relate the attack-free system states as *low pass graph signals* and FDIA event as *non low pass signals* [33]. Subsequently, Algorithm 1 can be applied regardless of error in topology estimation. To fix idea, a power network is described by $G = (V, E)$ such that V is the set of buses, and E is the set of transmission lines between buses. Let $\mathbf{Y} \in \mathbb{C}^{N \times N}$ be the admittance matrix such that $Y_{i,j} = 0$ if $(i, j) \notin E$. In quasi-steady state at time t , we observe the voltage phasors \mathbf{v}_t which can be approximated as the output of a low pass graph filter $\mathcal{H}(\mathbf{Y})$ with the excitation \mathbf{x}_t [33, Lemma 1]:

$$\mathbf{v}_t \approx \mathcal{H}(\mathbf{Y})\mathbf{x}_t + \mathbf{w}_t = (d\mathbf{I} + \mathbf{Y})^{-1}\mathbf{x}_t + \mathbf{w}_t, \quad (26)$$

where $d \in \mathbb{C}$ is a scalar that depends on \mathbf{Y} and $\mathbf{w}_t \in \mathbb{C}^N$ captures the slow time-varying nature of the model. On the other hand, the observed \mathbf{v}_t under FDIA is:

$$\mathbf{v}_{t,\text{FDI}} \approx \mathcal{H}(\mathbf{Y})\mathbf{x}_t + \delta_t + \mathbf{w}_t, \quad (27)$$

where δ_t models a possibly sparse attack signal [34], i.e., not low pass in general. Lastly, under the assumption that an FDIA event will persist for several samples, Algorithm 1 can be applied to batches of the voltage phasor graph signals to yield a *topology-free* FDIA detector. We envision that such a detector may be used in conjunction with existing algorithms such as [33], [34] for efficient detection of FDIA.

VI. NUMERICAL EXPERIMENTS

A. Detecting Low Pass Graph Signals

We consider synthetic graph signals on generated random graphs to verify our analysis result. The graph signals are generated according to (4) with the excitation given by $\mathbf{x}_m \in \mathbb{R}^N \sim N(\mathbf{0}, \mathbf{I})$ and the observation/modeling noise follows $\mathbf{w}_m \sim N(\mathbf{0}, \sigma^2\mathbf{I})$. For the experiments on non-modular graphs (with $K = 1$), we generate G as an Erdos-Renyi graph with connection probability of $p_{\text{er}} = 2 \log(N)/N$; for experiments with $K \geq 2$ clusters, we generate the graphs according to $G \sim \text{SBM}(K, N, \log(N)/N, 4 \log(N)/N)$. To benchmark the detection performance, we consider the classes for low pass or non low pass graph filters $\mathcal{H}(\mathbb{S})$ with the hypothesis $\mathcal{T}_0 : e^{-\tau L_{\text{norm}}}$ and $\mathcal{T}_1 : e^{\tau L_{\text{norm}}}$, where $\tau > 0$ is a parameter controlling the sharpness of the filters. We also compare with a two-step detection scheme based on SpecTemp [28] (via the fast implementation by [66]) which first learns a GSO from the stationary graph signals, and then verify if the graph signals are low pass using Definition 1. All experiments are conducted with 100 Monte-Carlo trials.

The first experiment concentrates on the case with $K = 1$ and evaluates the missed detection (MD) rate, $\Pr(\hat{\mathcal{T}} = \mathcal{T}_1 | \mathcal{T}_0)$, and false alarm (FA) rate, $\Pr(\hat{\mathcal{T}} = \mathcal{T}_0 | \mathcal{T}_1)$ against M and N respectively in Fig. 5 (left) and (right). We fixed $(N, \sigma^2) = (120, 0.01)$ in Fig. 5 (left) and $(M, \sigma^2) = (1000, 0.01)$ in Fig. 5 (right). As expected from Theorem 1, larger M and graph filters with sharper cutoffs (controlled by τ) reduce the error rate; while larger N raises the error rate. Compared to the benchmark scheme based on SpecTemp [28] and checking

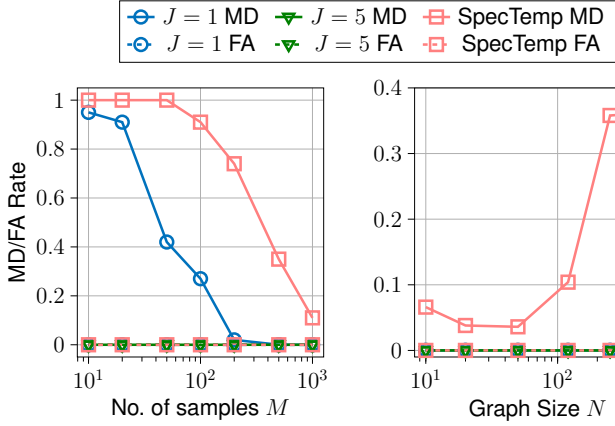


Fig. 5: **Error performance for detecting 1-low pass graph signals** against (Left) sample size M , (Right) graph size N . We set $J = 1$ for the experiment with SpecTemp [28].

Definition 1, Algorithm 1 achieves a lower MD rate at the same number of samples, and is less sensitive to graph size.

The second experiment considers the case with $K \geq 2$ and the filter parameter is fixed at $\tau = 0.6$. As the threshold δ in Algorithm 1 trades off between the false alarm and missed detection rates, we measure the detection performance through the AUROC score. Fig. 6 (top) show the performance of Algorithm 1 against M while setting $(N, \sigma^2) = (120, 0.01)$, and N while setting $(M, \sigma^2) = (0.01N^2, 0.01)$. Note that in the latter case, we set $M = \Theta(N^2)$ to compensate for the increase of signal dimension [cf. (20)]. Again as predicted by Theorem 2, we observe that the detection performance improves ($\text{AUROC} \rightarrow 1$) as M, N increase. Additionally, we consider a case when K is unknown and is estimated using the heuristic in Remark 1. Observe that the performance has only dropped slightly. Compared to the benchmark scheme based on SpecTemp [28], we observe improved performance across different sample and graph sizes for the proposed Algorithm 1.

The third experiment considers the sensitivity of Algorithm 1 to the filter's sharpness and the modularity of the graphs. We fix $\sigma^2 = 0.01$, $N = 120$, $M = 50$, and $r = \log N/N$. Fig. 6 (bottom) plots the AUROC performance of Algorithm 1 against the filter's parameter τ while setting $p = 4 \log N/N$, and against the graph's modularity p while setting $\tau = 0.6$. Observe the detection performance of Algorithm 1 improves as τ (filter's sharpness) increases and p (modularity) increases, confirming the analysis in Sec. IV.

Finally, we verify the robustness of Algorithm 1 to the graph topology on an actual network that is *not generated by the SBM*, and detecting via graph signals that are not excited by *white* input graph signal. This setup violates some of the assumptions required by our analysis. We consider the Political Books network [available: <http://www.orgnet.com/>] with $N = 105$ nodes and $|E| = 441$ edges, as illustrated in Fig. 7 (left). The graph has roughly $K = 2$ clusters.

We consider $R \in \{10, 25\}$ sources simulated as exogeneous sources of excitation to the graph. Accordingly, the input signals to the graph filter is generated as $\mathbf{x}_m = \mathbf{B}\mathbf{z}_m, \mathbf{z}_m \in \mathbb{R}^R \sim N(\mathbf{0}, \mathbf{I})$, where \mathbf{B} is a sparse bipartite graph with

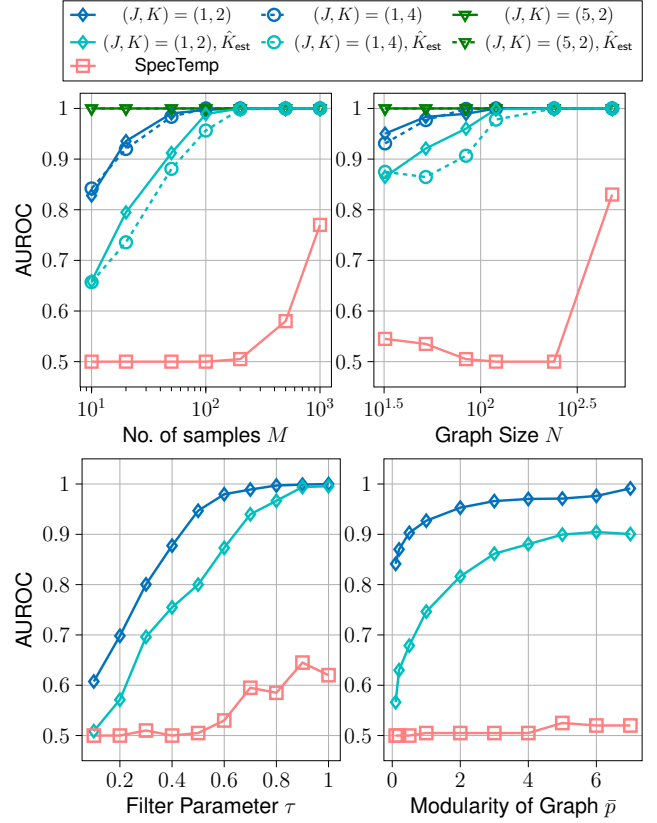


Fig. 6: **AUROC performance** against (Top-Left) sample size M ; (Top-Right) graph size N , where we set $J = 1, K = 2$ for the experiments with SpecTemp [28]; (Bottom-Left) filter's parameter τ ; (Bottom-Right) SBM parameter \bar{p} such that $p = \bar{p} \log N/N$. In the above, \hat{K}_{est} refers to the heuristics in Remark 1 which estimates K from data.

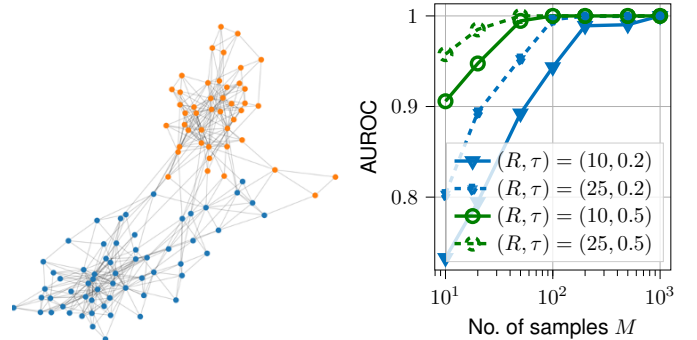


Fig. 7: **Political Books network**. (Left) The graph topology with $K = 2$ clusters. (Right) AUROC performance against M with Algorithm 1.

connectivity $2 \log N/N$ between the R sources and the existing N nodes on the graph. The low and high pass graph filters are respectively generated as $\mathcal{H}(\mathbb{S}) = (\mathbf{I} + \tau_2 \mathbf{L}_{\text{norm}})^{-1}$ and $\mathcal{H}(\mathbb{S}) = \mathbf{I} + \tau_2 \mathbf{L}_{\text{norm}}$. Fig. 7 (right) shows the AUROC performance against the number of samples M collected. Observe that $\text{AUROC} \rightarrow 1$ as M, R increase. The result illustrates that despite not all assumptions in Theorem 2 are satisfied, Algorithm 1 remains effective in tackling Problem 1.

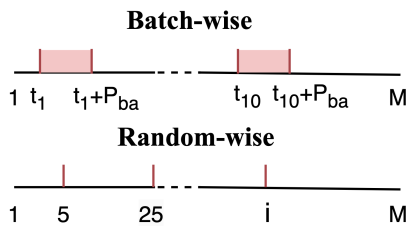


Fig. 8: **Batch-mode and random-mode pollution**, where red part indicates the positions of corrupted signals

B. Application Examples

This subsection illustrates numerical results from applying the proposed low pass detection algorithm to (I) robustify graph topology learning from corrupted signals, (II) detecting antagonistic behavior in social networks, (III) detecting anomaly status in power systems.

1) *Robustifying Graph Topology Learning*: Consider application (I) via pre-screening with Algorithm 1. We aim to evaluate the approach on synthetic graph models and signals. Particularly, we simulate a graph with $N = 20$ nodes, $G \sim \text{SBM}(2, N, \log(N)/N, 2 \log(N)/N)$, and the graph filter is given by $e^{\mathbf{L}^{\text{norm}}}$. The number of samples and observation noise variance are $(M, \sigma^2) = (2000, 0.01)$. To describe $\mathcal{M}_{\text{pollut}}$, we simulate signals that are corrupted in a batch-mode manner, or are corrupted uniformly at random. For the batch-mode setting, among the M samples, we randomly select ten time indices $\{t_1, \dots, t_{10}\}$ as the starting time for signal corruption. Subsequent signals are randomly contaminated in batches with the duration $M_{\text{ba}} \geq 1$, as illustrated by Fig. 8 (top). In other words, we have $\mathcal{M}_{\text{pollut}} = \cup_{i=1}^{10} \{t_i, \dots, t_i + M_{\text{ba}} - 1\}$. The uniform corruption setting is similar to the above where $\mathcal{M}_{\text{pollut}}$ is selected by randomly picking 10% of the indices from $\{1, \dots, 2000\}$, as illustrated by Fig. 8 (bottom).

We evaluate the graph topology learnt using GL-SigRep or SpecTemp combined with the proposed pre-screening scheme by Algorithm 1 (denoted ‘Pre-screen GL-SigRep/SpecTemp’). As benchmarks, we also compare with Inpaint model [55], OR-GL [57], LS-PGD [56], the plain GL-SigRep [54] and SpecTemp [28]. Note that the last two algorithms are not designed for graph topology learning with corrupted signals. The performance of graph learning is assessed via AUROC score. For the pre-screening procedure, we divide the graph signal dataset into batches of $m_{\text{batch}} = 50$ samples, and apply Algorithm 1 with the threshold δ . The Inpaint model [55] and the OR-GL [57] underwent 20 Monte-Carlo trials each, whereas the remaining simulations were conducted with at least 200 Monte-Carlo trials.

We test the graph learning performance under batch-mode corruption. Fig. 9 (left) shows the graph learning performance against the density of sparse noise p_s while fixing the contamination duration $M_{\text{ba}} = 20$. For each $m \in \mathcal{M}_{\text{pollut}}$, the corrupted signal $\mathbf{p}_m = \mathcal{H}(\mathbb{S})\mathbf{x}_m + \Delta\mathbf{p}_m$ is generated by contaminating the low pass signal $\mathcal{H}(\mathbb{S})\mathbf{x}_m$ with missed observations and sparse outlier noise, the latter is modeled using a sparse vector $\Delta\mathbf{p}_m$ – 10% of the entries will be missed and a $p_s N$ -sparse noise will be added with uniformly selected coordinates. For the sparse noise, its non-zero entries are

sampled from $\mathcal{N}(3\delta_y, 0.2\delta_y)$ with $\delta_y = \max_m \|\mathcal{H}(\mathbb{S})\mathbf{x}_m\|_\infty$. The latter model is designed such that the contaminated graph signals can evade detection by simple schemes such as thresholding on magnitudes. Moreover, Algorithm 1 with $K = 2$ is applied with $\delta = 0.8$. In the figure, we observe that the pre-screened GL-SigRep scheme achieves competitive graph learning performance especially when p_s is large. The performance improvement is significant compared to original GL-SigRep. The pre-screening procedure robustifies graph learning against outliers corruption (22). Additionally, Fig. 9 (mid-left) follows the same simulation setting as Fig. 9 (left) with $p_s = 0.5$. This figure demonstrates a performance tradeoff when deciding the batch size m_{batch} of the pre-screening procedure. We observe that the optimal m_{batch} is around 20-80 which is in the same order as $M_{\text{ba}} = 20$.

The second example considers batch-mode corruption with the outlier signal model taken from LS-PGD in [56, Eq. (5)]. Here, the outlier model includes both *uncertainty and noise*: for any $m \in \mathcal{M}_{\text{pollut}}$, we have $\mathbf{y}_m \sim \mathcal{N}(\boldsymbol{\mu}^*, \mathbb{S}^\dagger + \mathbf{I})$ where $\boldsymbol{\mu}^* \sim \mathcal{N}(\mathbf{0}, \mathbf{I})$. Fig. 9 (mid-right) compares the graph learning performance against the corruption duration M_{ba} , where we applied the pre-screened GL-SigRep scheme with the threshold $\delta = 0.6$. Observe that the pre-screened scheme delivers favorable performance across the tested range of M_{ba} .

Lastly, Fig. 9 (right) compares the performance of graph learning under the uniform corruption setting with a 10% contamination rate. The other simulation setting follows from Fig. 9 (left). Note that this setting favors OR-GL [57]. We observe that the pre-screened GL-SigRep scheme performs worse, yet it still outperforms the other benchmarks such as directly applying GL-SigRep on the corrupted data.

2) *Detecting Antagonistic Ties in Opinion Dynamics*: As discussed in Sec. V, opinion data tend to appear as low pass (resp. high pass) when the social network is dominated by friendly (resp. antagonistic) ties. This observation inspires us to use the normalized score $\text{score}_{\text{Alg1}} := \frac{1}{K} \mathbb{K}(\hat{\mathbf{U}}_K)$ in Algorithm 1 to measure the strength of antagonistic ties. As benchmarks, we compare two signed graph learning methods: GLASSO in [58], and the method in [60]. The two methods learn the weighted signed graph. To quantify the strength of antagonistic ties, we consider the normalized score

$$\text{score}_{\text{GL}} = \frac{\|\mathbf{A}_{E^-}\|_{\text{F}}}{\|\|\mathbf{A}_{E^+}\| + \|\mathbf{A}_{E^-}\|\|_{\text{F}}}, \quad (28)$$

such that \mathbf{A}_{E^-} , \mathbf{A}_{E^+} denote the adjacency matrix of negative, positive edges learnt, respectively. For ease of comparison, these scores are normalized to the range $[0, 1]$, where a smaller (larger) value suggests more friendly (antagonistic) ties⁴.

Our first experiment aims at verifying the above application of Algorithm 1 on synthetic data. We set $G \sim \text{SBM}(2, N, \log(N)/N, 4 \log(N)/N)$ with $N = 100$ nodes. The observation noise satisfies $\sigma^2 = 0.01$ and we consider generating $M = 200$ samples using the model in (24) with

⁴We acknowledge that as the goal for Algorithm 1 is different from [58], [60] by nature, it is impossible to make a completely fair comparison. Our examples serve as a reference to demonstrate that the proposed detector for antagonistic ties produce reasonable result with little computation overhead.

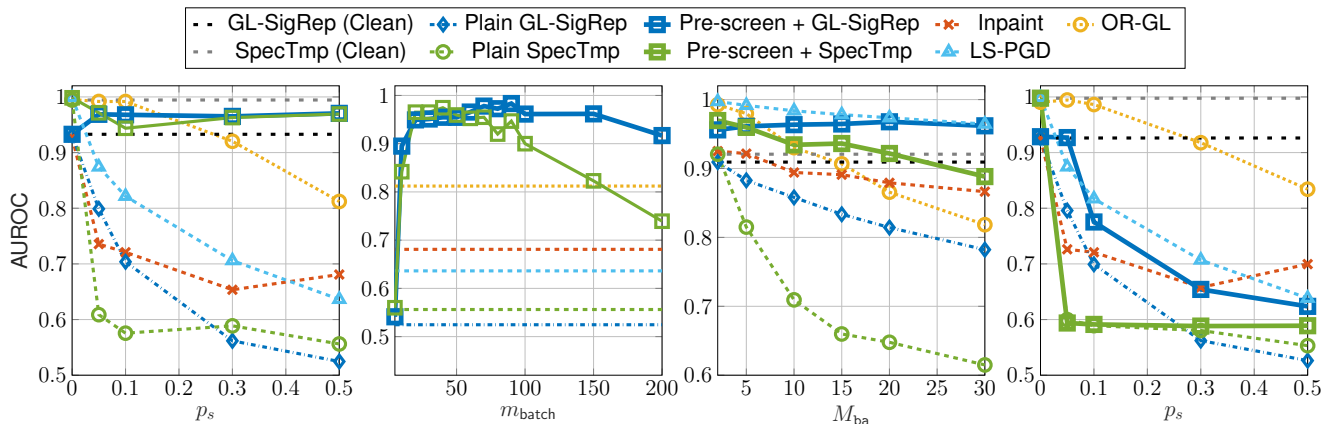


Fig. 9: **AUROC performance under polluted/corrupted data.** AUROC (left) against sparsity of outlier p_s under batch-mode pollution with sparse pollution; (Middle-left) against batch size M_{batch} under batch-mode pollution with sparse pollution at $p_s = 0.5$. (Middle-right) against size of corrupted batch M_{ba} under batch-mode pollution with [56]’s model. (Right) against sparsity of outlier p_s under random-mode pollution.

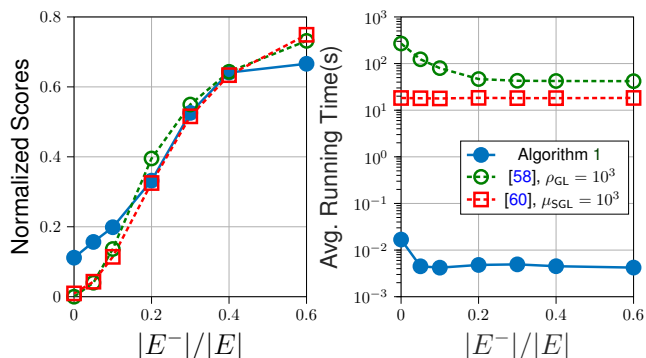


Fig. 10: **Synthetic Signed Graph.** (Left) Normalized scores of detecting antagonistic ties against $|E^-|/|E|$. (Right) Average runtime against $|E^-|/|E|$.

$\alpha = 0.8$ and $\mathbf{B} = \mathbf{I}$. For GLASSO, we pick the regularization parameter as $\rho_{\text{GL}} = 1000$, and for [60], we pick $\mu_{\text{SGL}} = 1000$. Fig. 10 compares $\text{score}_{\text{Alg1}}$, score_{GL} and the average runtime against the portion of negative edges in the ground truth graph where a portion of $|E^-|/|E|$ edges are randomly flipped to negative, with 50 Monte-Carlo trials. All algorithms detect the increased portion of antagonistic ties in the ground truth signed graphs, as indicated by the increasing detection scores as $|E^-|/|E| \rightarrow 1$. Algorithm 1 has a significantly lower runtime than other benchmarks.

Next, we apply Algorithm 1 to a US Senate rollcall dataset. The dataset is taken from the 117th US Congress [available: <https://voteview.com>], recording $M = 949$ rollcalls of votes made by $N = 97$ members. The M rollcalls are divided into 4 groups based on the attribute ‘vote question’ as: ‘‘On the Nomination’’, ‘‘On the Cloture Motion’’, ‘‘On the Amendment’’ and others. Each group is exemplified by rollcalls of different nature, as shown in Table I. We postulate that the Senators’ networks exhibit different levels of antagonistic ties in each of the group. For example, the opinion formation process on nomination of government positions (‘‘On the Nomination’’) may display more distrusts as opposed to the process on modifying a bill (‘‘On the Amendment’’).

On the Nomination (N): e.g., ‘‘Thomas J. Vilsack, of Iowa, to be Secretary of Agriculture’’, ‘‘Rahm Emanuel, of Illinois, to be Ambassador to Japan’’, ...
On the Cloture Motion (C): e.g., ‘‘Beth Robinson, of Vermont, to be United States Circuit Judge for the Second Circuit’’, ‘‘Douglas R. Bush, of Virginia, to be an Assistant Secretary of the Army’’, ...
On the Amendment (A): e.g., ‘‘To establish a deficit-neutral reserve fund relating to COVID-19 vaccine administration and a public awareness campaign’’, ‘‘In the nature of a substitute’’, ‘‘To improve the bill’’, ...
Others (O): e.g., ‘‘A bill to provide for reconciliation pursuant to title II of S. Con. Res. 5’’, ‘‘A resolution impeaching Donald John Trump, President of the United States, for high crimes and misdemeanors’’, ...

| | N | C | A | O |
|---|-------------|-------------|-------------|-------------|
| Algorithm 1 (0.08 sec.) | 0.37 | 0.39 | 0.02 | 0.06 |
| [58], $\rho_{\text{GL}} = 10$ (3969.92 sec.) | 0.14 | 0.18 | 0.05 | 0.10 |
| [58], $\rho_{\text{GL}} = 150$ (586.48 sec.) | 0.20 | 0.25 | 0.0 | 0.06 |
| [60], $\mu_{\text{SGL}} = 300$ (108.21 sec.) | 0.05 | 0.01 | 0.0 | 0.0 |
| [60], $\mu_{\text{SGL}} = 1000$ (124.28 sec.) | 0.17 | 0.22 | 0.0 | 0.07 |
| [60], $\mu_{\text{SGL}} = 2000$ (116.16 sec.) | 0.29 | 0.37 | 0.01 | 0.18 |

TABLE I: **Detecting Antagonistic Ties in US Senate Dataset.** (Left) Examples of rollcall descriptions in each group. (Right) Normalized scores, $\text{score}_{\text{Alg1}}$, score_{GL} , computed from the rollcalls of each group (see below). The bracketed numbers are the total computation time for each algorithm.

We process the data by assigning a score of $+1, 0, -1$ for a ‘Yay’, ‘Abstention’, ‘Nay’ vote, respectively, and set the number of clusters to $K = 2$ since there are two major parties. Table I shows the normalized scores (28) computed from the 4 groups of rollcalls. Observe that for Algorithm 1, the normalized K-means scores are significantly higher for the group with ‘‘On the Nomination’’, ‘‘On the Cloture Motion’’. This indicates that the graph filter processes involved are *non low pass* and shows traces of antagonistic ties. This is reasonable due to the common perception that these rollcalls are often contestable, even among the Senators of the same political party. On the other hand, the K-means score is lower for ‘‘On the Amendment’’, indicating the prevalence of *low pass* processes as the Senators tend to reach consensus for these rollcalls. Meanwhile, the graph learning methods are sensitive to the regularization parameters $\rho_{\text{GL}}, \lambda_{\text{SGL}}$.

Lastly, we apply Algorithm 1 to synthetic data generated from a real-world graph. Consider the highland-tribes graph [available: <http://konect.cc/networks/ucidata-gama/>] with $N + R = 16$ agents and $|E^+| = 29$, $|E^-| = 29$ edges, from which we select $R = 5$ agents as stubborn agents. We simulate the opinion dynamics by (23) and generate $M = 15$ samples with varying (dis)trust parameter $\alpha > 0$. The number

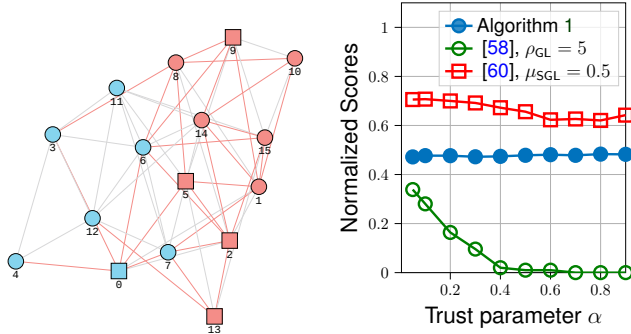


Fig. 11: **Highland tribes network.** (Left) The network: the red and grey lines are negative and positive edges, and the $R = 5$ rectangular nodes are the excitation nodes selected. (Right) Score against trust parameter $\alpha \in (0, 1)$ [cf. (23)].

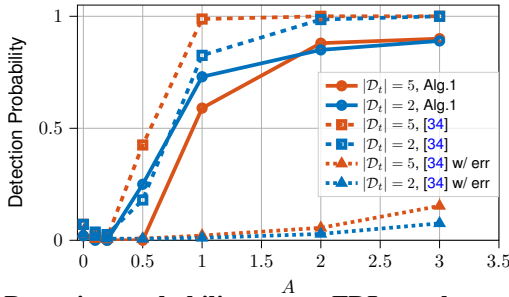


Fig. 12: **Detection probability versus FDI attack magnitude A_t .** We use ‘w/ err’ for [34] with perturbed topology, $|D_t|$ is the no. of attacked buses.

of the clusters in the graph is estimated as $K = 2$. Fig. 11 (right) shows the normalized scores of benchmark algorithms against α . Observe that the scores with Algorithm 1 and [60] are bounded away from zero consistently regardless of α , indicating the detection of antagonistic ties. Meanwhile, GLASSO [58] fails to recognize the antagonistic ties when $\alpha > 0.4$. We speculate that this is due to the effects of low-rank excitation in the synthetic graph signals.

3) *Detecting Anomalies in Power Systems:* Consider the voltage phasor data on an IEEE-118 bus test grid [available: <https://zenodo.org/record/5816149>]. The attack model is (27) with sparse attack vector δ_t such that $[\delta_t]_k = -Ae^{j\alpha_t}$ with the attack angle α_t uniformly distributed in $[0, 5^\circ]$.

Fig. 12 shows the detection probability versus the attack magnitude $A \in [0, 3]$ and different number of attacked buses $|D_t|$. We compare Algorithm 1 (assumed $K = 2$) against the detection method in [34] which requires knowledge of the network topology. Although the power network is a man-made system, its topology may not be correctly estimated when energized [65]. As such, we evaluate the performance when the graph topology is perturbed with 5% of random edge connection/disconnection. On the other hand, Algorithm 1 is a blind method that is robust to topology error. For the experiment, the detection probability is averaged over 100 trials and Algorithm 1 is set to use 100 samples per detection. Our results demonstrate that Algorithm 1 successfully detects FDIA events, and its performance is comparable to [34], despite not relying on topology information.

VII. CONCLUSIONS

This paper has initiated the study of a blind detection problem for low pass or smooth graph signals. The problem is motivated by the need to validate low-passness of graph signals before they can be used in GSP pipelines such as graph topology learning. We derive a detector that is inspired by the unique spectral pattern manifested by low pass graph signals defined on modular graphs and analyze their finite-sample complexity. Lastly, we discuss the applications of the proposed detectors on robustifying graph learning and anomaly detection in opinion dynamics data, power system data. Future works include extending the current method to directed graphs, studying applications to other domains and performance analysis on general modular graphs.

APPENDIX

A. Useful Lemmas

Below we state three useful results that will be instrumental to the subsequent analysis in this appendix.

Lemma 1. [30, Lemma 3.1] For $G \sim \text{SBM}(K, N, r, p)$, we have $\mathcal{A} = \mathbb{E}[\mathbf{A}] = \mathbf{Z}\mathbf{P}\mathbf{Z}^\top$, where $\mathbf{P} = p\mathbf{I}_K + r\mathbf{1}_K\mathbf{1}_K^\top$ and $\mathbf{Z} \in \{0, 1\}^{N \times K}$ is the cluster membership matrix. Moreover, $\mathcal{A}_{\text{norm}} = \mathcal{D}^{-1/2}\mathcal{A}\mathcal{D}^{-1/2}$ and $\mathcal{L}_{\text{norm}} = \mathbf{I} - \mathcal{A}_{\text{norm}}$, where $\mathcal{D}_{ii} = \sum_{j=1}^N \mathcal{A}_{ij}$. The eigenvectors that correspond to the smallest K eigenvalues of $\mathcal{L}_{\text{norm}}$ are given by

$$\mathcal{V}_K = \mathbf{Z}(\mathbf{Z}^\top\mathbf{Z})^{-1/2}\mathcal{U}, \quad (29)$$

where $\mathcal{U} \in \mathbb{R}^{K \times K}$ is an orthogonal matrix.

Lemma 2. Let $G \sim \text{SBM}(K, N, r, p)$ with $p \geq r > 0$ and $\frac{p}{K} + r \geq \frac{32 \log N + 1}{N}$, let $\mathbf{V}_K, \mathcal{V}_K$ denote the columns of the first K eigenvectors of $\mathbf{L}_{\text{norm}}, \mathcal{L}_{\text{norm}}$. Then, with probability at least $1 - 2/N$, there exists an orthogonal matrix $\mathcal{O}_K \in \mathbb{R}^{K \times K}$:

$$\|\mathbf{V}_K - \mathcal{V}_K\mathcal{O}_K\|_F \leq \sqrt{2}\|\sin \Theta(\mathbf{V}_K, \mathcal{V}_K)\|_F \leq \frac{35\sqrt{K^3 \log N}}{\sqrt{p(N-K)}}.$$

The proof is relegated to Appendix F. The conditions on p, r, K pertain to the difference between inter- and intra-cluster connection probabilities. The following lemma is obtained by combining [67, Theorem 2.1] and Davis-Kahan theorem:

Lemma 3. If $\Delta_{K,K} > 0$, there exists an orthogonal matrix $\hat{\mathcal{O}}_K$ such that with probability at least $1 - 5/M$,

$$\frac{1}{\sqrt{2}}\|\mathbf{U}_K\hat{\mathcal{O}}_K - \hat{\mathbf{U}}_K\|_F \leq \|\sin \Theta(\hat{\mathbf{U}}_K, \mathbf{U}_K)\|_F \leq \frac{2\sqrt{K}}{\Delta\beta_K}E_M$$

where c_1 is an absolute constant independent of N, M and

$$E_M := 2c_1\sqrt{\log M/M} \text{tr}(\mathbf{C}_y) + \sigma^2. \quad (30)$$

B. Proof of Proposition 1

We first show that \mathbf{v}_1 is a positive vector regardless of the choice of GSO. When $\mathbb{S} = \mathbf{L}$, $\mathbb{S} = \mathbf{L}_{\text{norm}}$, it is known that $\mathbf{v}_1 = \mathbf{1}/\sqrt{N}$, $\mathbf{v}_1 = \mathbf{D}^{1/2}\mathbf{1}/\|\mathbf{D}^{1/2}\mathbf{1}\|_2 > \mathbf{0}$, respectively; see [68, p. 4-7]. When $\mathbb{S} = \mathbf{A}$, $\mathbb{S} = \mathbf{A}_{\text{norm}}$, we note that

both matrices are non-negative. The Perron-Frobenius theorem implies \mathbf{v}_1 is a positive vector [69, Theorem 8.4.4].

Note that in all cases, the graph frequency λ_1 which corresponds to \mathbf{v}_1 has a multiplicity of one. As such, to show that \mathbf{v}_1 is the *only* positive eigenvector, it follows from the fact that every vector orthogonal to a positive vector must have at least one positive and negative element.

C. Proof of Proposition 2

For $\mathbf{N} \in \mathbb{R}^{N \times M}$, the K -means score (10) can be expressed via searching for K centroid vectors $\bar{\mathbf{n}}_1, \dots, \bar{\mathbf{n}}_K \in \mathbb{R}^M$:

$$\mathbb{K}(\mathbf{N}) = \min_{\bar{\mathbf{n}}_1, \dots, \bar{\mathbf{n}}_K \in \mathbb{R}^M} \sum_{\ell=1}^N \min_{j=1, \dots, K} \|\mathbf{n}_\ell - \bar{\mathbf{n}}_j\|^2. \quad (31)$$

Define the set

$$\mathcal{R}_K^{N \times M} = \{\bar{\mathbf{N}} \in \mathbb{R}^{N \times M} : \text{no. of unique rows of } \bar{\mathbf{N}} \leq K\}.$$

It is easy to observe that

$$\mathbb{K}(\mathbf{N}) = \min_{\bar{\mathbf{N}} \in \mathcal{R}_K^{N \times M}} \|\mathbf{N} - \bar{\mathbf{N}}\|_{\text{F}}^2. \quad (32)$$

To bound $\mathbb{K}(\mathbf{V}_K)$, we invoke Lemma 2 and consider the population eigenvector matrix $\mathcal{V}_K \mathcal{O}_K$ defined therein. Notice that as $\mathcal{V}_K \in \mathcal{R}_K^{N \times K}$ [cf. (29)] and \mathcal{O}_K is a $K \times K$ orthogonal matrix, we have $\mathcal{V}_K \mathcal{O}_K \in \mathcal{R}_K^{N \times K}$. By Lemma 2, the following holds with probability at least $1 - 2/N$,

$$\begin{aligned} \mathbb{K}(\mathbf{V}_K) &= \min_{\bar{\mathbf{V}} \in \mathcal{R}_K^{N \times K}} \|\mathbf{V}_K - \bar{\mathbf{V}}\|_{\text{F}}^2 \leq \|\mathbf{V}_K - \mathcal{V}_K \mathcal{O}_K\|_{\text{F}}^2 \\ &\leq (p(N - K))^{-1} 35^2 K^3 \log N. \end{aligned} \quad (33)$$

D. Proof of Theorem 1

To simplify notation, we assume without loss of generality that $\|\hat{\mathbf{u}}_i - (\hat{\mathbf{u}}_i)_+\|_1 \leq \|\hat{\mathbf{u}}_i + (-\hat{\mathbf{u}}_i)_+\|_1$ for any $i = 1, \dots, N$. Therefore, the positivity function is simplified to

$$\text{Pos}(\hat{\mathbf{u}}_i) = \|\hat{\mathbf{u}}_i - (\hat{\mathbf{u}}_i)_+\|_1.$$

We proceed by bounding $\text{Pos}(\hat{\mathbf{u}}_i)$ under different cases:

1) When $\mathcal{T}_{\text{gnd}} = \mathcal{T}_0$: We have $\mathbf{u}_1 = \mathbf{v}_1 > \mathbf{0}$ and

$$\text{Pos}(\hat{\mathbf{u}}_1) \leq \|\hat{\mathbf{u}}_1 - \mathbf{u}_1\|_1 + \|\mathbf{u}_1 - (\mathbf{u}_1)_+\|_1 = \|\hat{\mathbf{u}}_1 - \mathbf{u}_1\|_1.$$

where we used $|\min\{a, 0\} - \min\{b, 0\}| \leq |a - b|$ for any $a, b \in \mathbb{R}$. For any $j \geq 2$, similarly we have:

$$\text{Pos}(\hat{\mathbf{u}}_j) \geq \|\mathbf{u}_j - (\mathbf{u}_j)_+\|_1 - \|\hat{\mathbf{u}}_j - \mathbf{u}_j\|_1 \geq c_0 - \|\hat{\mathbf{u}}_j - \mathbf{u}_j\|_1, \text{ [cf. (38)],}$$

where we have used the fact that for any $j \geq 2$, it holds $\mathbf{u}_j = \mathbf{v}_{j'}$ for some $2 \leq j' \leq N$.

2) When $\mathcal{T}_{\text{gnd}} = \mathcal{T}_1$: As $\mathcal{H}(\mathbb{S})$ is *not* 1-low pass, it holds

$$\text{Pos}(\hat{\mathbf{u}}_1) \geq \|\mathbf{u}_1 - (\mathbf{u}_1)_+\|_1 - \|\hat{\mathbf{u}}_1 - \mathbf{u}_1\|_1 \geq c_0 - \|\hat{\mathbf{u}}_1 - \mathbf{u}_1\|_1$$

since $\mathbf{u}_1 = \mathbf{v}_{j'}$ for some $2 \leq j' \leq N$. Meanwhile, there exists $j^* \in \{2, \dots, N\}$ such that $\mathbf{u}_{j^*} = \mathbf{v}_1 > \mathbf{0}$. We also bound

$$\begin{aligned} \min_{j=2, \dots, N} \text{Pos}(\hat{\mathbf{u}}_j) &\leq \left\| \hat{\mathbf{u}}_{j^*} - (\hat{\mathbf{u}}_{j^*})_+ \right\|_1 \\ &\leq \left\| \mathbf{u}_{j^*} - (\mathbf{u}_{j^*})_+ \right\|_1 + \|\hat{\mathbf{u}}_{j^*} - \mathbf{u}_{j^*}\|_1 = \|\hat{\mathbf{u}}_{j^*} - \mathbf{u}_{j^*}\|_1. \end{aligned} \quad (34)$$

From the above discussions, a sufficient condition for the detector to be accurate, i.e., $\hat{\mathcal{T}} = \mathcal{T}_{\text{gnd}}$, is

$$c_0 \geq 2 \max_{j=1, \dots, N} \|\hat{\mathbf{u}}_j - \mathbf{u}_j\|_1. \quad (35)$$

Applying Lemma 3 with $K = 1$ yields

$$\max_{j=1, \dots, N} \|\mathbf{u}_j - \hat{\mathbf{u}}_j\|_1 \leq 2^{1.5} \sqrt{N} E_M / \Delta^{\min}, \quad (36)$$

where E_M is defined in (30) and the extra \sqrt{N} is due to norm equivalence. Rearranging terms conclude the proof.

E. Proof of Theorem 2

We proceed by bounding the sample complexity under different cases for \mathcal{T}_{gnd} .

1) When $\mathcal{T}_{\text{gnd}} = \mathcal{T}_0$: As $\mathcal{H}(\mathbb{S})$ is a K low pass graph filter, we observe that $\mathbf{U}_K = \mathbf{V}_K \Pi_K$ for some permutation matrix $\Pi_K \in \{0, 1\}^{K \times K}$. Define the orthogonal matrix $\bar{\mathcal{O}}_K = \mathcal{O}_K \Pi_K \hat{\mathcal{O}}_K$, where $\mathcal{O}_K, \hat{\mathcal{O}}_K$ are from Lemma 2, 3, respectively. It holds with probability at least $1 - 2/N - 5/M$,

$$\begin{aligned} \mathbb{K}(\hat{\mathbf{U}}_K) &\leq \|\hat{\mathbf{U}}_K - \mathcal{V}_K \bar{\mathcal{O}}_K\|_{\text{F}}^2 \\ &\leq 2 \|\hat{\mathbf{U}}_K - \mathbf{U}_K \hat{\mathcal{O}}_K\|_{\text{F}}^2 + 2 \|\mathbf{U}_K \hat{\mathcal{O}}_K - \mathcal{V}_K \bar{\mathcal{O}}_K\|_{\text{F}}^2 \\ &\leq 16K \left(\frac{E_M}{\Delta} \right)^2 + \frac{2450K^3 \log N}{p(N - K)}. \end{aligned} \quad (37)$$

2) When $\mathcal{T}_{\text{gnd}} = \mathcal{T}_1$: As $\mathcal{H}(\mathbb{S})$ is *not* K low pass, the columns of \mathbf{U}_K has at least one eigenvector from $\{\mathbf{v}_{K+1}, \dots, \mathbf{v}_N\}$.

To facilitate our analysis, we define the shorthand notations $\hat{\mathbf{U}}_{r,s} = [\hat{\mathbf{u}}_r, \dots, \hat{\mathbf{u}}_s]$, $\mathbf{U}_{r,s} = [\mathbf{u}_r, \dots, \mathbf{u}_s]$ where $r \leq s$. We also define the permutation function $\pi : \{1, \dots, N\} \rightarrow \{1, \dots, N\}$ such that $|h_i| = |h(\lambda_{\pi(i)})|$, where $\pi(i)$ is the index of graph frequency for the i th largest frequency response⁵ in $\mathcal{H}(\mathbb{S})$ and is well-defined under H2. Set

$$\mathcal{P}^{\text{high}} = \{i : 1 \leq i \leq K, K + 1 \leq \pi(i) \leq N\} \quad (38)$$

to be the set of *crossed* frequencies which is non-empty under $\mathcal{T}_{\text{gnd}} = \mathcal{T}_1$.

Let $\mathbf{O} \in \mathbb{R}^{K \times K}$ be an orthogonal matrix. From (32), we obtain that $\mathbb{K}(\mathbf{V}_K \mathbf{O}) = \min_{\mathbf{M} \in \mathcal{R}_K^{N \times K}} \|\mathbf{V}_K - \mathbf{M} \mathbf{O}^\top\|_{\text{F}}^2$. Since $\mathbf{M} \mathbf{O}^\top \in \mathcal{R}_K^{N \times K}$, we have $\mathbb{K}(\mathbf{V}_K \mathbf{O}) = \mathbb{K}(\mathbf{V}_K)$. This indicates that K -means score is invariant to multiplication by orthogonal matrices. For any $r \leq s$ with $[r, s] \subseteq \mathcal{P}^{\text{high}}$

$$\begin{aligned} \sqrt{\mathbb{K}(\hat{\mathbf{U}}_K)} &= \sqrt{\mathbb{K}(\hat{\mathbf{U}}_K \hat{\mathcal{O}}_K)} \\ &= \min_{\mathbf{M} \in \mathcal{R}_K^{N \times K}} \|\hat{\mathbf{U}}_K \hat{\mathcal{O}}_K - \mathbf{M}\|_{\text{F}} \\ &\geq \sqrt{\mathbb{K}(\mathbf{U}_K)} - \|\mathbf{U}_K - \hat{\mathbf{U}}_K \hat{\mathcal{O}}_K\|_{\text{F}} \\ &\geq \sqrt{\mathbb{K}(\mathbf{U}_{r,s})} - \|\mathbf{U}_K - \hat{\mathbf{U}}_K \hat{\mathcal{O}}_K\|_{\text{F}}. \end{aligned} \quad (39)$$

By the definition of $\mathcal{P}^{\text{high}}$, $\mathbf{U}_{r,s}$ consists of at least one vector from $\{\mathbf{v}_{K+1}, \dots, \mathbf{v}_N\}$. From H1, we have $\mathbb{K}(\mathbf{U}_{r,s}) \geq c_{\text{SBM}}$. It can be shown that (20) implies $\sqrt{c_{\text{SBM}}} > \frac{2^{3/2} \sqrt{K}}{\Delta} E_M$. Thus

⁵Recall that $|h_1| > \dots > |h_N|$ are sorted in descending order.

applying Lemma 3 shows that the following lower bound holds with probability at least $1 - 5/M$,

$$\mathbb{K}(\widehat{\mathbf{U}}_K) \geq \left(\sqrt{c_{\text{SBM}}} - \frac{2^{3/2}\sqrt{K}}{\Delta} E_M \right)^2. \quad (40)$$

Collecting (37), (40) and observe that $\widehat{\mathcal{T}} = \mathcal{T}_{\text{gnd}}$ is guaranteed if (i) δ upper bounds the RHS of (37), and (ii) δ lower bounds the RHS of (40). The proof is concluded.

F. Proof of Lemma 2

Let $\sin \Theta(\mathbf{V}_K, \mathcal{V}_K)$ be a diagonal matrix whose i th diagonal element is $\sin(\cos^{-1}(\sigma_i))$ and σ_i is the i th singular value of $\mathbf{V}_K^\top \mathcal{V}_K$. Notice that $\mathcal{L}_{\text{norm}} = \mathbf{I} - \mathcal{A}_{\text{norm}}$ and $\mathbf{L}_{\text{norm}} = \mathbf{I} - \mathbf{A}_{\text{norm}}$, we first apply the Davis-Kahan theorem [70] to bound the subspace difference between $\mathbf{V}_K, \mathcal{V}_K$:

$$\|\sin \Theta(\mathbf{V}_K, \mathcal{V}_K)\|_{\text{F}} \leq \frac{2\sqrt{K}\|\mathbf{A}_{\text{norm}} - \mathcal{A}_{\text{norm}}\|_2}{\lambda_K^{\mathcal{A}_{\text{norm}}} - \lambda_{K+1}^{\mathcal{A}_{\text{norm}}}}, \quad (41)$$

where $\lambda_j^{\mathcal{A}_{\text{norm}}}$ denotes the j th largest eigenvalue of $\mathcal{A}_{\text{norm}}$. Theorem 4 of [50] shows that when the minimum expected degree of nodes satisfies $d_{\min, N} \geq 32 \log N$, with probability at least $1 - 2/N$, it holds

$$\|\mathcal{A}_{\text{norm}} - \mathbf{A}_{\text{norm}}\|_2 \leq 10\sqrt{\log(N)/d_{\min, N}}. \quad (42)$$

We have $d_{\min, N} = \frac{N(p+rK)}{K} - (p+r)$. The condition $\frac{p}{K} + r \geq \frac{32 \log N + 1}{N}$ guarantees $d_{\min, N} \geq 32 \log N$. By [30, p. 34–37], we have $\lambda_K^{\mathcal{A}_{\text{norm}}} = \frac{p}{rK+p}$ and $\lambda_{K+1}^{\mathcal{A}_{\text{norm}}} = 0$. As such,

$$\begin{aligned} & \|\sin \Theta(\mathbf{V}_K, \mathcal{V}_K)\|_{\text{F}} \\ & \leq \frac{20\sqrt{K}\sqrt{\log N}}{\sqrt{\frac{N(p+rK)}{K} - (p+r)} \frac{p}{p+rK}} \leq \frac{25K^{1.5}\sqrt{\log N}}{\sqrt{p}\sqrt{N-K}}, \end{aligned} \quad (43)$$

Finally, we observe that with probability at least $1 - 2/N$,

$$\|\mathbf{V}_K - \mathcal{V}_K \mathcal{O}_K\|_{\text{F}} \leq \sqrt{2} \|\sin \Theta(\mathbf{V}_K, \mathcal{V}_K)\|_{\text{F}} \leq \frac{35K^{1.5}\sqrt{\log N}}{\sqrt{p}\sqrt{N-K}}.$$

REFERENCES

- [1] Y. He and H.-T. Wai, "Identifying first-order lowpass graph signals using perron frobenius theorem," in *ICASSP*, 2021.
- [2] M. Newman, *Networks*. Oxford university press, 2018.
- [3] M. J. Wainwright, M. I. Jordan *et al.*, "Graphical models, exponential families, and variational inference," *Foundations and Trends® in Machine Learning*, vol. 1, no. 1–2, pp. 1–305, 2008.
- [4] A. Ortega, P. Frossard, J. Kovačević, J. M. F. Moura, and P. Vandergheynst, "Graph signal processing: Overview, challenges, and applications," *Proceedings of the IEEE*, vol. 106, no. 5, pp. 808–828, 2018.
- [5] A. Sandryhaila and J. M. Moura, "Discrete signal processing on graphs," *IEEE transactions on signal processing*, 2013.
- [6] E. Isufi, F. Gama, D. I. Shuman, and S. Segarra, "Graph filters for signal processing and machine learning on graphs," *arXiv preprint arXiv:2211.08854*, 2022.
- [7] R. Ramakrishna, H. T. Wai, and A. Scaglione, "A user guide to low-pass graph signal processing and its applications: Tools and applications," *IEEE Signal Processing Magazine*, vol. 37, no. 6, pp. 74–85, 2020.
- [8] W. Huang, T. A. W. Bolton, J. D. Medaglia, D. S. Bassett, A. Ribeiro, and D. Van De Ville, "A graph signal processing perspective on functional brain imaging," *Proceedings of the IEEE*, 2018.
- [9] D. Thanou, X. Dong, D. Kressner, and P. Frossard, "Learning heat diffusion graphs," *IEEE Transactions on Signal and Information Processing over Networks*, vol. 3, no. 3, pp. 484–499, 2017.
- [10] X. Dong, D. Thanou, P. Frossard, and P. Vandergheynst, "Learning laplacian matrix in smooth graph signal representations," *IEEE Transactions on Signal Processing*, vol. 64, no. 23, pp. 6160–6173, 2016.
- [11] V. Kalofolias, "How to learn a graph from smooth signals," in *Artificial Intelligence and Statistics*. PMLR, 2016, pp. 920–929.
- [12] X. Dong, D. Thanou, M. Rabbat, and P. Frossard, "Learning graphs from data: A signal representation perspective," *IEEE Signal Processing Magazine*, vol. 36, no. 3, pp. 44–63, 2019.
- [13] G. Mateos, S. Segarra, A. G. Marques, and A. Ribeiro, "Connecting the dots: Identifying network structure via graph signal processing," *IEEE Signal Processing Magazine*, vol. 36, no. 3, pp. 16–43, 2019.
- [14] H.-T. Wai, S. Segarra, A. E. Ozdaglar, A. Scaglione, and A. Jadbabaie, "Blind community detection from low-rank excitations of a graph filter," *IEEE Transactions on Signal Processing*, vol. 68, pp. 436–451, 2020.
- [15] H.-T. Wai, Y. C. Eldar, A. E. Ozdaglar, and A. Scaglione, "Community inference from partially observed graph signals: Algorithms and analysis," *IEEE Transactions on Signal Processing*, 2022.
- [16] M. T. Schaub, S. Segarra, and J. N. Tsitsiklis, "Blind identification of stochastic block models from dynamical observations," *SIAM Journal on Mathematics of Data Science*, vol. 2, no. 2, pp. 335–367, jan 2020.
- [17] T. M. Roddenberry, M. T. Schaub, H.-T. Wai, and S. Segarra, "Exact blind community detection from signals on multiple graphs," *IEEE Transactions on Signal Processing*, 2020.
- [18] T. M. Roddenberry and S. Segarra, "Blind inference of eigenvector centrality rankings," *IEEE Transactions on Signal Processing*, 2021.
- [19] Y. He and H.-T. Wai, "Detecting central nodes from low-rank excited graph signals via structured factor analysis," *IEEE Transactions on Signal Processing*, 2022.
- [20] —, "Online inference for mixture model of streaming graph signals with sparse excitation," *IEEE Transactions on Signal Processing*, 2023.
- [21] J. Pang, G. Cheung, A. Ortega, and O. C. Au, "Optimal graph laplacian regularization for natural image denoising," in *ICASSP*, 2015.
- [22] A. Anis, A. Gadde, and A. Ortega, "Efficient sampling set selection for bandlimited graph signals using graph spectral proxies," *IEEE Transactions on Signal Processing*, vol. 64, no. 14, pp. 3775–3789, 2016.
- [23] H. NT and T. Maehara, "Revisiting graph neural networks: All we have is low-pass filters," *ArXiv*, vol. abs/1905.09550, 2019.
- [24] F. Wu, A. Souza, T. Zhang, C. Fifty, T. Yu, and K. Weinberger, "Simplifying graph convolutional networks," in *ICML*. PMLR, 2019.
- [25] A. Sandryhaila and J. M. Moura, "Discrete signal processing on graphs: Frequency analysis," *IEEE Transactions on Signal Processing*, vol. 62, no. 12, pp. 3042–3054, 2014.
- [26] P. Ferrer-Cid, J. M. Barcelo-Ordinas, and J. Garcia-Vidal, "Volterra graph-based outlier detection for air pollution sensor networks," *IEEE Transactions on Network Science and Engineering*, vol. 9, no. 4, pp. 2759–2771, 2022.
- [27] M. Wax and T. Kailath, "Detection of signals by information theoretic criteria," *IEEE Transactions on acoustics, speech, and signal processing*, vol. 33, no. 2, pp. 387–392, 1985.
- [28] S. Segarra, A. G. Marques, G. Mateos, and A. Ribeiro, "Network topology inference from spectral templates," *IEEE Transactions on Signal and Information Processing over Networks*, vol. 3, no. 3, pp. 467–483, 2017.
- [29] M. Girvan and M. E. Newman, "Community structure in social and biological networks," *Proceedings of the national academy of sciences*, vol. 99, no. 12, pp. 7821–7826, 2002.
- [30] K. Rohe, S. Chatterjee, and B. Yu, "Spectral clustering and the high-dimensional stochastic blockmodel," *The Annals of Statistics*, 2011.
- [31] T. Dittrich and G. Matz, "Signal processing on signed graphs: Fundamentals and potentials," *IEEE Signal Processing Magazine*, 2020.
- [32] C. Altafini, "Consensus problems on networks with antagonistic interactions," *IEEE Trans. Autom. Control*, vol. 58, no. 4, pp. 935–946, 2012.
- [33] R. Ramakrishna and A. Scaglione, "Grid-graph signal processing (grid-gsp): A graph signal processing framework for the power grid," *IEEE Transactions on Signal Processing*, vol. 69, pp. 2725–2739, 2021.
- [34] E. Drayer and T. Routtenberg, "Detection of false data injection attacks in smart grids based on graph signal processing," *IEEE Systems Journal*, vol. 14, no. 2, pp. 1886–1896, 2020.
- [35] M. Scholkemper and M. T. Schaub, "Blind extraction of equitable partitions from graph signals," in *ICASSP*, 2022, pp. 5832–5836.
- [36] L. Tong, G. Xu, and T. Kailath, "Blind identification and equalization based on second-order statistics: A time domain approach," *IEEE Transactions on information Theory*, vol. 40, no. 2, pp. 340–349, 1994.

- [37] B. Barzel and A.-L. Barabasi, “Universality in network dynamics,” *Nature physics*, vol. 9, p. 673–681, 11 2013.
- [38] H.-T. Wai, A. Scaglione, B. Barzel, and A. Leshem, “Joint network topology and dynamics recovery from perturbed stationary points,” *IEEE Transactions on Signal Processing*, vol. 67, no. 17, pp. 4582–4596, 2019.
- [39] Y. Zhu, F. J. I. Garcia, A. G. Marques, and S. Segarra, “Estimating network processes via blind identification of multiple graph filters,” *IEEE Transactions on Signal Processing*, vol. 68, pp. 3049–3063, 2020.
- [40] S. Segarra, G. Mateos, A. G. Marques, and A. Ribeiro, “Blind identification of graph filters,” *IEEE Transactions on Signal Processing*, vol. 65, no. 5, pp. 1146–1159, 2016.
- [41] M. E. Newman, “Spectral methods for community detection and graph partitioning,” *Physical Review E*, vol. 88, no. 4, p. 042822, 2013.
- [42] U. Von Luxburg, “A tutorial on spectral clustering,” *Statistics and computing*, vol. 17, pp. 395–416, 2007.
- [43] S. Deng, S. Ling, and T. Strohmer, “Strong consistency, graph laplacians, and the stochastic block model,” *The Journal of Machine Learning Research*, vol. 22, no. 1, pp. 5210–5253, 2021.
- [44] N. Perraudin and P. Vandergheynst, “Stationary signal processing on graphs,” *IEEE Transactions on Signal Processing*, vol. 65, no. 13, pp. 3462–3477, 2017.
- [45] A. G. Marques, S. Segarra, G. Leus, and A. Ribeiro, “Stationary graph processes and spectral estimation,” *IEEE Transactions on Signal Processing*, vol. 65, no. 22, pp. 5911–5926, 2017.
- [46] S.-Y. Yun and A. Proutiere, “Accurate community detection in the stochastic block model via spectral algorithms,” *arXiv preprint arXiv:1412.7335*, 2014.
- [47] J. Lei and A. Rinaldo, “Consistency of spectral clustering in stochastic block models,” *The Annals of Statistics*, vol. 43, no. 1, pp. 215–237, 2015.
- [48] A. Kumar, Y. Sabharwal, and S. Sen, “A simple linear time (1+ ϵ)-approximation algorithm for k-means clustering in any dimensions,” in *45th Annual IEEE Symposium on Foundations of Computer Science*. IEEE, 2004, pp. 454–462.
- [49] S. Ben-David and M. Ackerman, “Measures of clustering quality: A working set of axioms for clustering,” *Advances in neural information processing systems*, vol. 21, 2008.
- [50] A. Joseph and B. Yu, “Impact of regularization on spectral clustering,” *The Annals of Statistics*, vol. 44, no. 4, pp. 1765–1791, 2016.
- [51] A. Kadavankandy, L. Cottatellucci, and K. Avrachenkov, “Characterization of random matrix eigenvectors for stochastic block model,” in *2015 49th Asilomar Conference on Signals, Systems and Computers*. IEEE, 2015, pp. 861–865.
- [52] Z. Bai and G. Pan, “Limiting behavior of eigenvectors of large wigner matrices,” *Journal of Statistical Physics*, vol. 146, no. 3, pp. 519–549, 2012.
- [53] M. Fiedler, “A property of eigenvectors of nonnegative symmetric matrices and its application to graph theory,” *Czechoslovak Mathematical Journal*, vol. 25, no. 4, pp. 619–633, 1975.
- [54] X. Dong, D. Thanou, P. Frossard, and P. Vandergheynst, “Learning laplacian matrix in smooth graph signal representations,” *IEEE Transactions on Signal Processing*, vol. 64, no. 23, pp. 6160–6173, 2016.
- [55] P. Berger, G. Hannak, and G. Matz, “Efficient graph learning from noisy and incomplete data,” *IEEE Transactions on Signal and Information Processing over Networks*, vol. 6, pp. 105–119, 2020.
- [56] X. Wang, Y.-M. Pun, and A. M.-C. So, “Distributionally robust graph learning from smooth signals under moment uncertainty,” *IEEE Transactions on Signal Processing*, vol. 70, pp. 6216–6231, 2022.
- [57] H. Araghi and M. Babaie-zadeh, “An outlier-robust smoothness-based graph learning approach,” *Signal Processing*, p. 108927, 2023.
- [58] J. Friedman, T. Hastie, and R. Tibshirani, “Sparse inverse covariance estimation with the graphical lasso,” *Biostatistics*, vol. 9, no. 3, pp. 432–441, 2008.
- [59] C. Dinesh, G. Cheung, S. Bagheri, and I. V. Bajic, “Efficient signed graph sampling via balancing & gershgorin disc perfect alignment,” *arXiv preprint arXiv:2208.08726*, 2022.
- [60] G. Matz and T. Dittrich, “Learning signed graphs from data,” in *ICASSP 2020-2020 IEEE International Conference on Acoustics, Speech and Signal Processing (ICASSP)*. IEEE, 2020, pp. 5570–5574.
- [61] A. Karaaslanli, S. Saha, S. Aviyente, and T. Maiti, “scsgl: kernelized signed graph learning for single-cell gene regulatory network inference,” *Bioinformatics*, vol. 38, no. 11, pp. 3011–3019, 2022.
- [62] A. V. Proskurnikov and R. Tempo, “A tutorial on modeling and analysis of dynamic social networks. part ii,” *Annual Reviews in Control*, vol. 45, pp. 166–190, 2018.
- [63] D. Acemoglu, A. Ozdaglar, and A. ParandehGheibi, “Spread of (mis)information in social networks,” *Games and Economic Behavior*, vol. 70, no. 2, pp. 194–227, 2010.
- [64] P. Jia, A. MirTabatabaei, N. E. Friedkin, and F. Bullo, “Opinion dynamics and the evolution of social power in influence networks,” *SIAM Review*, vol. 57, no. 3, pp. 367–397, 2015.
- [65] G. Cavraro, V. Kekatos, and S. Veeramachaneni, “Voltage analytics for power distribution network topology verification,” *IEEE Transactions on Smart Grid*, vol. 10, no. 1, pp. 1058–1067, 2017.
- [66] R. Shafipour, A. Hashemi, G. Mateos, and H. Vikalo, “Online topology inference from streaming stationary graph signals,” in *2019 IEEE Data Science Workshop (DSW)*. IEEE, 2019, pp. 140–144.
- [67] F. Bunea and L. Xiao, “On the sample covariance matrix estimator of reduced effective rank population matrices, with applications to fPCA,” *Bernoulli*, vol. 21, no. 2, May 2015.
- [68] F. R. Chung, *Spectral graph theory*. American Mathematical Soc., 1997, vol. 92.
- [69] R. A. Horn and C. R. Johnson, *Matrix analysis*. Cambridge university press, 2012.
- [70] Y. Yu, T. Wang, and R. J. Samworth, “A useful variant of the davis—kahan theorem for statisticians,” *Biometrika*, vol. 102, 2015.
- [71] A. Gittens, P. Kambadur, and C. Boutsidis, “Approximate spectral clustering via randomized sketching,” *ArXiv*, vol. abs/1311.2854, 2013.

Supplementary Material for “Detecting Low Pass Graph Signals via Spectral Pattern: Sampling Complexity and Applications”

Chenyue Zhang, Yiran He, Hoi-To Wai

APPENDIX

This supplementary document showcases the applicability of Algorithm 1 for tackling Problem 1 with non-stationary graph signals, i.e., when $C_x = \mathbb{E}[\mathbf{x}_m \mathbf{x}_m^\top] \neq \mathbf{I}$.

(I) **Observation Model.** We examine a general model of non-white excitation where $\mathbf{x}_m = \mathbf{B} \mathbf{z}_m$. Without loss of generality, the latent parameter vector $\mathbf{z}_m \in \mathbb{R}^R$ follows a zero-mean, sub-Gaussian distribution with the covariance $\mathbb{E}[\mathbf{z}_m \mathbf{z}_m^\top] = \mathbf{I}$, and the matrix $\mathbf{B} \in \mathbb{R}^{N \times R}$, $R \leq N$. Note that this implies the excitation covariance $\mathbb{E}[\mathbf{x}_m \mathbf{x}_m^\top] = \mathbf{B} \mathbf{B}^\top$. The observed signal in Eq. (4) can be rewritten as:

$$\mathbf{y}_m = \underbrace{\mathcal{H}(\mathbb{S}) \cdots \mathcal{H}(\mathbb{S})}_{J_m \text{ times}} \mathbf{B} \mathbf{z}_m + \mathbf{w}_m, \quad m = 1, \dots, M, \quad (44)$$

with the noiseless signal covariance matrix:

$$\begin{aligned} \bar{\mathbf{C}}_y &= \frac{1}{J} \sum_{\tau=1}^J [\mathcal{H}(\mathbb{S})]^\tau \mathbf{B} \mathbf{B}^\top [\mathcal{H}(\mathbb{S})]^\tau \\ &= \mathbf{V} \left(\frac{1}{J} \sum_{\tau=1}^J h(\Lambda)^\tau \mathbf{V}^\top \mathbf{B} \mathbf{B}^\top \mathbf{V} h(\Lambda)^\tau \right) \mathbf{V}^\top. \end{aligned} \quad (45)$$

We now illustrate that (45) admits the spectral pattern described in Section III in an approximate fashion provided that the graph filters have sufficiently ‘sharp’ frequency responses (to be discussed later) and $K \leq R$. Note that this enables us to tackle Problem 1 using Algorithm 1. To keep the discussion simple, we focus on the case where $J = 1$. The noiseless covariance matrix can be written as:

$$\bar{\mathbf{C}}_y = \mathbf{V} (h(\Lambda) \mathbf{V}^\top \mathbf{B} \mathbf{B}^\top \mathbf{V} h(\Lambda)) \mathbf{V}^\top = \bar{\mathbf{U}} \boldsymbol{\beta} \bar{\mathbf{U}}^\top. \quad (46)$$

where $\boldsymbol{\beta} = \text{Diag}(\beta_1(\bar{\mathbf{C}}_y), \dots, \beta_N(\bar{\mathbf{C}}_y))$ is a diagonal matrix for the eigenvalues of $\bar{\mathbf{C}}_y$ sorted in descending order, and $\bar{\mathbf{U}}$ is the eigenvector matrix of $\bar{\mathbf{C}}_y$. We consider two hypothesis for $\mathcal{H}(\mathbb{S})$ as follows.

I) *When $\mathcal{T}_{\text{gnd}} = \mathcal{T}_0$:* Suppose that the graph filter is sufficiently ‘sharp’, i.e.,

$$\eta_K = \frac{\max\{|h(\lambda_{K+1})|, \dots, |h(\lambda_N)|\}}{\min\{|h(\lambda_1)|, \dots, |h(\lambda_K)|\}} \ll 1. \quad (47)$$

In this case, we have the approximation

$$\bar{\mathbf{C}}_y \approx \mathbf{V}_K (h(\Lambda_K) \mathbf{V}_K^\top \mathbf{B} \mathbf{B}^\top \mathbf{V}_K h(\Lambda_K)) \mathbf{V}_K^\top.$$

The authors are with the Department of SEEM, The Chinese University of Hong Kong, Shatin, Hong Kong SAR of China. E-mails: czhang@se.cuhk.edu.hk, yrhe@se.cuhk.edu.hk, htwai@se.cuhk.edu.hk. This work is supported in part by CUHK Direct Grant #4055135 and HKRGC Project #24203520.

Consequently, it can be deduced that the top- K eigenvectors, $\hat{\mathbf{U}}_K$, of the observation covariance matrix satisfies $\text{span}(\hat{\mathbf{U}}_K) \approx \text{span}(\mathbf{V}_K)$. It follows that both $\mathbb{K}(\hat{\mathbf{U}}_K)$, $\text{Pos}(\hat{\mathbf{u}}_1)$ will be small when $\mathcal{T}_{\text{gnd}} = \mathcal{T}_0$.

2) *When $\mathcal{T}_{\text{gnd}} = \mathcal{T}_1$:* Similar to the previous case, we require the graph filter to satisfy the following sharpness condition:

$$\frac{|h_{K+1}|}{|h_K|} = \frac{|h(\lambda_{\pi(K+1)})|}{|h(\lambda_{\pi(K)})|} \ll 1, \quad (48)$$

where we recall the definition of $\pi(\cdot)$ such that $|h_i| = |h(\lambda_{\pi(i)})|$ and $|h_i|$ is the i th highest frequency response of the graph filter. Similarly, we observe that $\bar{\mathbf{C}}_y$ is approximated by

$$\mathbf{V}_{\pi(\{[K]\})} \left(h(\Lambda_{\pi(\{[K]\})}) \mathbf{V}_{\pi(\{[K]\})}^\top \mathbf{B} \mathbf{B}^\top \mathbf{V}_{\pi(\{[K]\})} h(\Lambda_{\pi(\{[K]\})}) \right) \mathbf{V}_{\pi(\{[K]\})}^\top$$

Consequently, the set of top- K eigenvectors, $\hat{\mathbf{U}}_K$, of the observed covariance matrix satisfies $\text{span}(\hat{\mathbf{U}}_K) \approx \text{span}(\mathbf{V}_{\pi(\{[K]\})})$. Since $\mathbf{V}_{\pi(\{[K]\})}$ contains an eigenvector \mathbf{v}_i with $i \in \mathcal{P}^{\text{high}}$ (38), it follows that $\mathbb{K}(\hat{\mathbf{U}}_K)$, $\text{Pos}(\hat{\mathbf{u}}_1)$ are likely to be bounded away from zero when $\mathcal{T}_{\text{gnd}} = \mathcal{T}_1$.

The above derivation shows that if the admissible graph filters are sufficiently sharp, i.e., satisfying (47), (48), then Algorithm 1 is applicable to non-stationary graph signals with general excitation (44). Note that this differs from the analysis for stationary graph signals in Section III, IV, where the sharpness of graph filters only affects the sample complexity of the algorithm. To give further insight, we conclude this supplementary document by quantifying the effects of the sharpness of graph filters under finite number of samples.

(II) **Performance Analysis when $\mathbf{B} \neq \mathbf{I}$.** For simplicity, we further concentrate on applying Algorithm 1 with $K \geq 2$. Our techniques can be readily extended to other cases such as when $J \geq 2$ or $K = 1$. To fix ideas, the eigenvalues of $\mathcal{H}(\mathbb{S})$ are arranged in descending order as $|h_1| > \dots > |h_N|$. The *strength* (a.k.a. sharpness) of the graph filter at the i th graph frequency is defined as $\bar{\eta}_i := |h_{i+1}|/|h_i|$. When $\mathcal{H}(\mathbb{S})$ is K -low pass, we observe that $\bar{\eta}_K$ coincides with the low pass ratio $\bar{\eta}_K = \eta_K < 1$.

We consider a mild condition for \mathbf{B} and $\mathcal{H}(\mathbb{S})$. Let \mathbf{Q}_K be the top- K right singular vectors of $\mathcal{H}(\mathbb{S})\mathbf{B}$. We require:

H3. Assume: (i) $\text{rank}(\mathcal{H}(\mathbb{S})\mathbf{B}) \geq K$, (ii) $\beta_K > \beta_{K+1}$, and (iii) $\text{rank}(\mathbf{U}_K^\top \mathbf{B} \mathbf{Q}_K) = K$.

We recall that $\beta_i := \beta_i(\overline{\mathbf{C}}_y)$ as defined in (46). The above conditions are relatively mild, e.g., they typically hold when \mathbf{B} has full column rank.

Note that the eigenvectors of $\overline{\mathbf{C}}_y$ are now *perturbed* version for the columns of $\{\mathbf{v}_1, \dots, \mathbf{v}_N\}$. Recall that \mathbf{U}_K is the top- K eigenvectors of the noiseless covariance $\overline{\mathbf{C}}_y$ of the *stationary graph signals* in (4), our first step is to control the difference between \mathbf{U}_K and $\overline{\mathbf{U}}_K$:

Lemma 4. *Fix $1 \leq K \leq R$, and assume H3. There exists an orthogonal matrix $\overline{\mathbf{O}}_K$ such that*

$$\|\overline{\mathbf{U}}_K - \mathbf{U}_K \overline{\mathbf{O}}_K^\top\|_F^2 \leq \bar{\eta}_K^2 2K\mathbb{B}. \quad (49)$$

where $\mathbb{B} = \|\mathbf{U}_{N-K}^\top \mathbf{B} \mathbf{Q} \mathbf{Q}_K\|_2^2 \|(\mathbf{U}_K^\top \mathbf{B} \mathbf{Q} \mathbf{Q}_K)^{-1}\|_2^2$.

Proof. Applying [14, Proposition 1], we obtain

$$\|\mathbf{U}_K(\mathbf{U}_K)^\top - \overline{\mathbf{U}}_K \overline{\mathbf{U}}_K^\top\|_2^2 \leq \bar{\eta}_K^2 \mathbb{B}. \quad (50)$$

From [71, Lemma 7], we then have $\|\overline{\mathbf{U}}_K - \mathbf{U}_K \overline{\mathbf{O}}_K\|_F \leq \sqrt{2K} \|\mathbf{U}_K \mathbf{U}_K^\top - \overline{\mathbf{U}}_K \overline{\mathbf{U}}_K^\top\|_2$. This concludes the proof. \square

Note that in the above, we have $\mathbb{B} = 0$ if $\mathbf{B} = \mathbf{I}$. The above lemma leads to the following theorem on the finite sample performance of Algorithm 1:

Theorem 3. *Let $G \sim \text{SBM}(K, N, r, p)$ with $p \geq r > 0$, $\frac{p}{K} + r \geq \frac{32 \log N + 1}{N}$, H3 holds, and take $\mathbb{S} = \mathbf{L}_{\text{norm}}$ as the unweighted adjacency matrix. Accordingly, let*

$$\begin{aligned} \overline{\Delta} &:= \inf_{\Delta \beta_K: \mathcal{H}(\mathbb{S}) \in \mathcal{H}_s^{\text{low}} \cup \mathcal{H}_s^{\text{hi}}} \Delta \beta_K, \quad \bar{\eta}_K := \sup_{\bar{\eta}_K: \mathcal{H}(\mathbb{S}) \in \mathcal{H}_s^{\text{low}} \cup \mathcal{H}_s^{\text{hi}}} \bar{\eta}_K, \\ \delta_1 &:= \sqrt{\frac{\delta}{2} - \frac{1225K^3 \log N}{p(N-K)} - 2K\bar{\eta}^2 \mathbb{B}}, \\ \delta_2 &:= \sqrt{c_{\text{sbm}}} - \sqrt{2K\mathbb{B}\bar{\eta}} - \sqrt{\delta}, \end{aligned}$$

Assume that $\overline{\Delta} > 0$, $\bar{\delta}_{\min} := \min\{\delta_1, \delta_2\} > 0$, and the noise variance $\sigma^2 \leq \bar{\delta}_{\min} \overline{\Delta} / \sqrt{8K}$. If it holds that

$$\sqrt{\frac{M}{\log M}} \geq \frac{2c_1 \text{tr}(\mathbf{C}_y)}{\bar{\delta}_{\min} \overline{\Delta} / \sqrt{8K} - \sigma^2}, \quad (51)$$

then

$$\Pr(\widehat{\mathcal{T}} = \mathcal{T}_{\text{gnd}}) \geq 1 - 10/M - 2/N. \quad (52)$$

Proof. We proceed by modifying the proof of Theorem 2 in appendix E.

1) When $\mathcal{T}_{\text{gnd}} = \mathcal{T}_0$: Define the orthogonal matrices $\tilde{\mathbf{O}}_K = \overline{\mathbf{O}}_K \widehat{\mathbf{O}}_K$, $\tilde{\theta}_K = \theta_K \Pi_K \widehat{\mathbf{O}}_K$, where $\theta_K, \widehat{\mathbf{O}}_K, \overline{\mathbf{O}}_K$ are from Lemma 2, 3, 4, respectively. Combining (37) with lemma 4, it holds with probability at least $1 - 2/N - 5/M$ that

$$\begin{aligned} \mathbb{K}(\widehat{\mathbf{U}}_K) &\leq \|\widehat{\mathbf{U}}_K - \mathcal{V}_K \tilde{\theta}_K\|_F^2 \\ &\leq 2\|\widehat{\mathbf{U}}_K - \overline{\mathbf{U}}_K \widehat{\mathbf{O}}_K\|_F^2 + 2\|\overline{\mathbf{U}}_K \widehat{\mathbf{O}}_K - \mathbf{U}_K \tilde{\theta}_K\|_F^2 \\ &\quad + 2\|\mathbf{U}_K \tilde{\theta}_K - \mathcal{V}_K \tilde{\theta}_K\|_F^2 \\ &\leq 16K \left(\frac{E_M}{\Delta}\right)^2 + 4K\bar{\eta}^2 \mathbb{B} + \frac{2450K^3 \log N}{p(N-K)}. \end{aligned} \quad (53)$$

2) When $\mathcal{T}_{\text{gnd}} = \mathcal{T}_1$: Combining (39) with Lemma 4, we have

$$\begin{aligned} \sqrt{\mathbb{K}(\widehat{\mathbf{U}}_K)} &= \sqrt{\mathbb{K}(\widehat{\mathbf{U}}_K \widehat{\mathbf{O}}_K)} \\ &\geq \sqrt{\mathbb{K}(\overline{\mathbf{U}}_K)} - \|\overline{\mathbf{U}}_K - \widehat{\mathbf{U}}_K \widehat{\mathbf{O}}_K\|_F \\ &\geq \sqrt{\mathbb{K}(\mathbf{U}_K \overline{\mathbf{O}}_K)} - \|\mathbf{U}_K \overline{\mathbf{O}}_K - \overline{\mathbf{U}}_K\|_F - \|\overline{\mathbf{U}}_K - \widehat{\mathbf{U}}_K \widehat{\mathbf{O}}_K\|_F \\ &\geq \sqrt{\mathbb{K}(\mathbf{U}_{r,s})} - \|\mathbf{U}_K \overline{\mathbf{O}}_K - \overline{\mathbf{U}}_K\|_F - \|\overline{\mathbf{U}}_K - \widehat{\mathbf{U}}_K \widehat{\mathbf{O}}_K\|_F \end{aligned}$$

As it can be shown from (51) that $\sqrt{c_{\text{SBM}}} > \frac{2^{3/2}\sqrt{K}}{\Delta} E_M + \bar{\eta}_K \sqrt{2K\mathbb{B}}$, we have the following lower bound that holds with probability at least $1 - 5/M$,

$$\mathbb{K}(\widehat{\mathbf{U}}_K) \geq \left(\sqrt{c_{\text{SBM}}} - \frac{2^{3/2}\sqrt{K}}{\Delta} E_M - \bar{\eta} \sqrt{2K\mathbb{B}} \right)^2. \quad (54)$$

Collecting (53), (54) concludes the proof. \square

The above result highlights a salient difference between the case of non-stationary graph signals (44) and stationary graph signals (4) considered in the main paper. Particularly, satisfying the assumptions in Theorem 3 necessitates $\sqrt{c_{\text{SBM}}} > \sqrt{2K\mathbb{B}}\bar{\eta}$. That is, the sharpness of the graph filters in consideration has to be higher than a certain threshold specified by the non-clusterability of the bulk eigenvectors, *regardless* of the number of sample observed and the noise variance. This restriction is not found in the case of stationary graph signals Theorem 2, and it can be understood from the intuition that follows (47), (48). In particular, when $\bar{\eta} \approx 1$, the approximation of the top- K eigenvectors in $\overline{\mathbf{C}}_y$ as $\mathbf{V}_{\pi([K])}$ is no longer valid and the top- K eigenvectors in $\overline{\mathbf{C}}_y$ suffers from an *intrinsic perturbation* from $\mathbf{V}_{\pi([K])}$ due to the effects of the matrix \mathbf{B} .